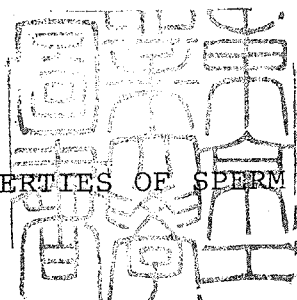


論文 / 著書情報
Article / Book Information

題目(和文)	
Title(English)	Mechanical Properties of Sperm Flagella
著者(和文)	石島純夫
Author(English)	SUMIO ISHIJIMA
出典(和文)	学位:理学博士, 学位授与機関:東京工業大学, 報告番号:甲第1451号, 授与年月日:1983年3月26日, 学位の種別:課程博士, 審査員:
Citation(English)	Degree:Doctor of Science, Conferring organization: , Report number:甲第1451号, Conferred date:1983/3/26, Degree Type:Course doctor, Examiner:
学位種別(和文)	博士論文
Type(English)	Doctoral Thesis

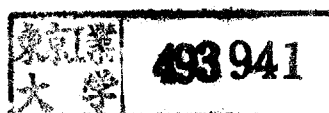
A-29

MECHANICAL PROPERTIES OF SPERM FLAGELLA



Sumio Ishijima

Department of Applied Physics
Tokyo Institute of Technology



CONTENTS

	Page
INTRODUCTION	1
CHAPTER I. FLEXURAL RIGIDITY OF SEA URCHIN SPERM FLAGELLA	7
CHAPTER II. FLEXURAL RIGIDITY OF MAMMALIAN SPERM FLAGELLA	50
CHAPTER III. MOVEMENT CHARACTERISTICS OF HAMSTER SPERMATOZOA	68
REFERENCES	83
ACKNOWLEDGMENT	86

INTRODUCTION

In large organisms, the muscle is main motor apparatus for locomotion. However, ameboid, ciliary, and flagellar movements are the main means of locomotion in small organisms. Even in large organisms, cilia and flagella are used for generating local movements in their bodies, e.g. movement of mucus in trachea. There appears to be no fundamental difference in structure and mechanism between a cilium (plural cilia) and a flagellum (plural flagella). Cilia generally occur in large numbers on a cell, whereas flagella generally occur single or in a few numbers.

Using a microscope designed by himself, Leeuwenhoek first observed beating cilia in ciliated protozoa in 1675. Cilia and flagella are found in all the animal kingdom and some in plant kingdom, while they are not found in prokaryote. Bacterial flagella are different from eukaryotic flagella and cilia structurally as well as functionally.

The structure of cilia and flagella has been known by improvements in the techniques for electron microscopy. As shown in Fig.1, the fundamental structure of flagella and cilia consists of 9 peripheral doublet microtubules and 2 singlet central microtubules. The "9+2" pattern is typical of the majority of cilia and flagella. The plane of beat is perpendicular to the plane including the two central tubules.

A pair of projections from each doublet microtubule called "arms" are present. The outer and inner arms on each doublet have different profiles, with the outer arms

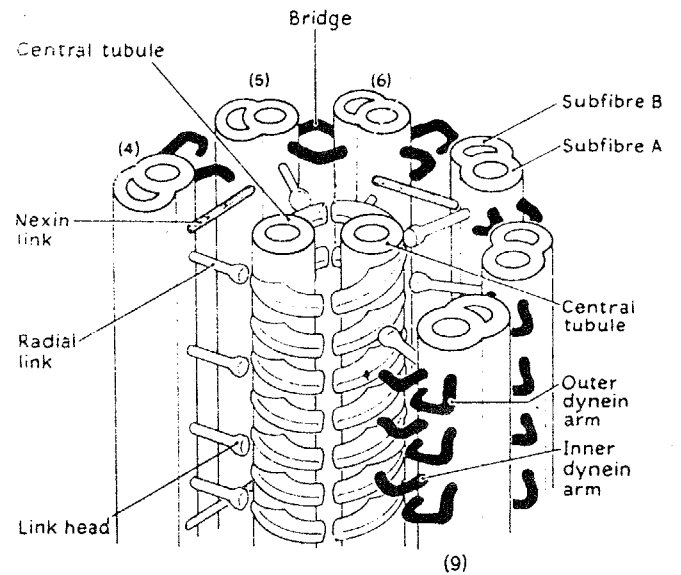
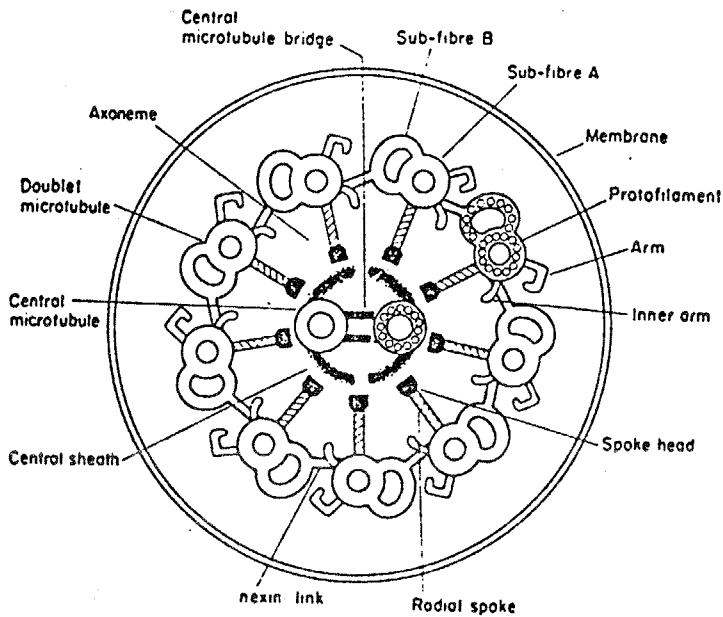


Fig.1. Diagram showing the structure of the flagellum.

(a) Cross section of the flagellum as viewed from base to tip.

(b) Schematic diagram of the axoneme structure. The base of the axoneme is toward the top of the page; outer doublets 1,2 and 3 are removed.

terminating in a hook-like bend, whereas the inner arm curves gently inward and has no terminal end. The arms, which are present repeatedly at a longitudinal periodicity of about 24 nm, consist of a protein, dynein having ATPase activity. The microtubules of the axoneme consist of globular protein molecules (diameter 4 nm) called tubulin arranged in tubular form as shown in Fig.1. Central microtubules are complete tubule having 13 filaments each of which consists of an array of tubulin molecules. The outer nine doublets consist of subfiber A, complete tubule having 13 tubulin molecules in cross section and subfiber B, incomplete C-type tubule composed of 10 tubulin molecules in cross section.

The radial spokes are rigid structures attached perpendicularly to the A tubules and connecting the central sheath and outer doublet microtubules. The nexin links connecting adjacent doublet microtubules are highly elastic: Although their normal length is about 30 nm, they can be stretched to as much as 250 nm. The longitudinal periodicity of the nexin links is about 96 nm. Central sheath is composed of two rows of projections arising from each central-pair tubule. The central tubules are connected by intermicrotubule bridges.

In the sperm flagella of mammals, gastropods, and many insects, the axoneme is surrounded by nine outer coarse fibers as shown in Fig.2. Whether the nine outer coarse fibers are passive structures or whether they contribute actively to flagellar motility is controversial. Phillips (1972) show that, among mammals, the sperm flagella having

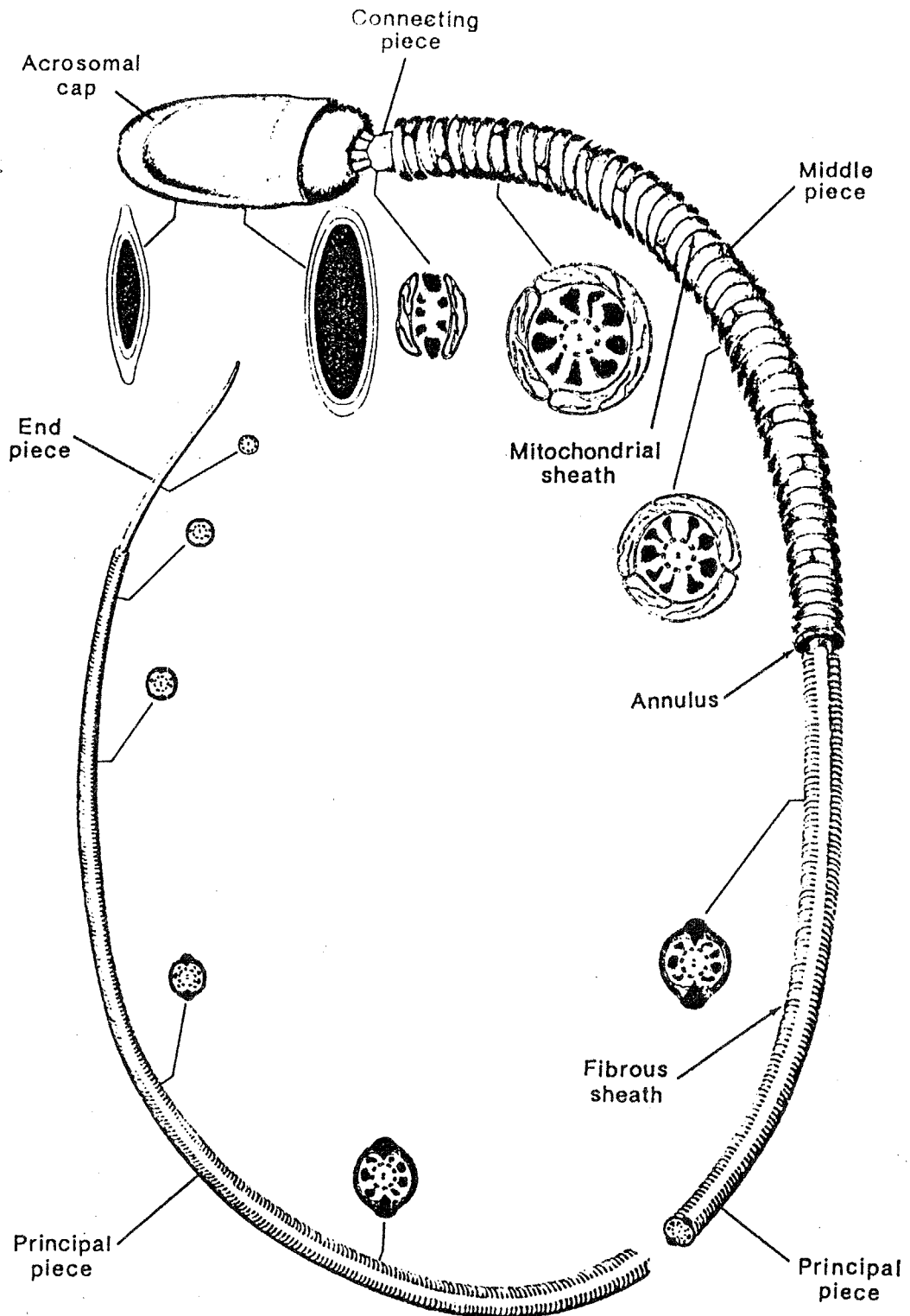


Fig.2. Diagram of a typical mammalian spermatozoon.

The cell membrane is removed to reveal the underlying structural components. Running through the axis of the sperm tail for its entire length is the axoneme, a longitudinal bundle of microtubules similar to that found in cilia and flagella in general. Outside of the axoneme is a row of nine longitudinally oriented outer coarse flbers.

thick outer coarse fibers has a relatively low amplitude of the beating flagella and suggested that these fibers are major factors in flagellar stiffness; they are composed of a keratin-like protein with no detectable ATPase activity.

Gray (1955) found that beating of spermatozoa of marine invertebrates, such as sea urchins, is nearly planar, that planar bending waves are propagated along their lengths at a beat frequency of 30-40 Hz, and that at certain stages of the beat cycle the flagellum showed a form of sine curve. Subsequent analysis of sea urchin sperm flagellar movement by Brokaw (1965) who used stroboscopic flashes for recording, indicated that the waveform could be represented more accurately by a series of circular arcs joined by short, straight segments than by a simple sine curve. The studies of mammalian (bull) spermatozoa (Gray 1958) showed that the amplitude of bending flagella increases progressively along the tail toward the distal end, and that the movement in the proximal region is planar.

Gray and Hancock (1955) developed a simple computation method based upon expressing the viscous force acting on a short segment of flagellum in terms of normal and tangential components of the resistance. They were then able to show that the forward velocity of the sperm computed from the observed flagellar waveform and frequency was in good agreement with that actually observed, and also to show that the viscous drag of the sperm head was small compared with that of the flagellum.

Hoffmann-Berling (1955) showed that when the cell

membrane has been destroyed by treatment with 50% glycerol and then ATP was added to it, flagellum was reactivated to move. Gibbons and Gibbons (1972) discovered that improved reactivation system could be obtained by using a nonionic detergent, Triton X-100 (polyoxyethylene isooctylphenol ether) which completely removed the membranes from the flagella of sea urchin spermatozoa. The resulting demembranated spermatozoa become essentially 100% motile when subsequently reactivate with ATP, and their flagellar beat is very similar to that of live spermatozoa.

Satir (1965,1968) has shown that the microtubules of the axoneme slide past each other during bending of the ciliary shaft by careful electron microscopic examination. Summers and Gibbons (1971) obtained a conclusive evidence for the occurrence of active sliding between flagellar tubules: Triton-demembranated flagellar axonemes were isolated from sea urchin sperm and were digested briefly with trypsin. When ATP was added, the axoneme disintegrated into doublet microtubules. Observation by dark-field light microscopy showed that this disintegration occurred by extrusion of tubules from the axoneme by a gradual sliding process and that the length, after disintegration was complete, ranged up to eight times that of the original axonemal fragment. Examination of the trypsin digestion as a function of time showed that the dynein arms generate active shearing stress between adjacent doublet tubules.

FLEXURAL RIGIDITY OF SEA URCHIN SPERM FLAGELLA

Introduction

In echinoderm sperm flagella, planar bending waves are initiated at the base of the flagellum and propagate toward the tip. In the beating flagellum, the active bending force generated in it, the passive resistance due to the deformation of the internal structures and the viscous drag of the external fluid applied to the flagellum balance with one another because the Reynolds number in the present motion system is very small. Therefore, the measurement of mechanical properties of flagella during movement is important in elucidation of the mechanism of flagellar movement. Baba (1972) determined the flexural rigidity of compound cilia on Mytilus gill from the force applied to the beating cilium with a microneedle and the instantaneous change in the curvature of the ciliary shaft by the force. Okuno and Hiramoto (1979) measured the stiffness of motionless echinoderm sperm flagella from the force applied to the flagellum with a microneedle and the bending of the flagellum caused by the force. Okuno (1980) investigated the effect of vanadate on the stiffness of demembranated flagella by the same method and found that the flagella are in a relaxed state in the presence of MgATP^{2-} and vanadate.

In the present study, flexural rigidity of sea urchin sperm flagella during beating and in motionless state was determined from the deformation of the flagellum caused

by the stream of the medium and the viscous resistance of the medium acting on the flagella calculated by hydrodynamic theories. Effects of demembration with triton X-100, digestion of nexin links and radial spokes with trypsin, inhibition of dynein ATPase with vanadate or erythro-9-[3-2-(Hydroxynonyl)] adenine [EHNA] and concentration of ATP on the flexural rigidity of the flagellum were also examined, in order to investigate contributions of structures constituting the flagellum, such as cell membrane, outer doublet microtubules, nexin links, dynein arms, radial spokes and central singlet microtubules, to the flexural rigidity of flagella in rest as well as during beating.

Materials and Methods

Spermatozoa were obtained from the sea urchins, Clypeaster japonicus and Pseudocentrotus depressus, by intracoelomic injection of 1 mM acetylcholine dissolved in artificial sea water [ASW] (Jamarin U, Jamarin Laboratory, Osaka) in the case of Clypeaster japonicus and of 0.5 M KCl in the case of Pseudocentrotus depressus. Undiluted semen was stored in a refrigerator, and used within 2-3 hours after the spawning. In the experiments with living beating flagella, the semen was diluted to 10^6 times with ASW. In order to immobilize the sperm flagella, the semen was diluted to 10^3 times with ASW and then this sperm suspension

was diluted 10^3 times with CO_2 -saturated artificial sea water [CO_2 -ASW]. It was confirmed, after experimentation, that these immobilized spermatozoa recovered their motility when they were transferred to normal ASW as reported by Okuno and Hiramoto (1979). In some experiments the sperm flagella ceased their motility in the ASW containing 2 mM erythro-9-[3-2-(Hydroxynonyl)] adenine [EHNA] (Burroughs Wellcome, Research Triangle Park, NC). It was confirmed that the inhibition of flagellar motility by EHNA could be reversed by 10 times dilution of the sperm suspension with normal ASW (cf. Bouchard, Penningroth, Cheung, Gagnon and Bardin 1981).

In experiments using demembranated spermatozoa, membranes of spermatozoa were removed according to the method of Gibbons and Gibbons (1972) with minor modifications. One volume of sperm suspension prepared by 10^3 times dilution of the semen with ASW was mixed with 20 volumes of extracting solution (0.04% w/v Triton X-100, 0.15 M KCl, 4 mM MgSO_4 , 0.5 mM ethylene diamine tetra acetate [EDTA], 0.5 mM dithiothreitol [DDT], pH 8.0 by 2 mM tris-hydroxymethylaminomethane [Tris]-HCl buffer). The mixture was gently agitated for 30 s at room temperature.

These demembranated spermatozoa were diluted 50 times with reactivating solution [0.15 M KCl, 2 mM MgSO_4 , 0.5 mM EDTA, 2 μM -1 mM ATP, 5 mM DTT, 2% polyethyleneglycol [PEG], ml.wt=20,000, Nakarai Chemicals.LTD. Kyoto, pH 8.0 by 20 mM Tris-HCl buffer] were used for experiments. In the experiments of demembranated flagella poisoned with vanadate

or EHNA, the demembranated flagella reactivated with 1 mM ATP were put into solution containing 10 μ M sodium orthovanadate (Wako Pure Chemical Industries, LTD., Tokyo) or 2 mM EHNA in the reactivating solution mentioned above. After the measurements, the recovery of flagellar beating was checked by adding 2 mM norepinephrine (Sigma Chemical Co., St. Louis, MO) (cf. Fagen and Racker 1977) to the medium in the case of the sperm flagella immobilized with sodium orthovanadate. In the case of the sperm flagella immobilized with EHNA, the recovery of flagellar activity was checked by diluting the medium with normal reactivating solution by 10 times. Viscosity of ASW measured with an Ostwald type capillary viscometer was 1.1×10^{-3} Pa.s and viscosity of the reactivating solution and that of the ATP-free medium was 2.5×10^{-3} Pa.s. Trypsin-digested demembranated flagella were prepared by treating the demembranated flagella obtained by the above methods into a solution containing 100 μ g/ml trypsin (E. Merck AG., Darmstadt) (0.15 M KCl, 2 mM MgSO_4 , 0.5 mM EDTA, 5 mM DTT, 2% PEG, 20 mM Tris-HCl buffer pH 8.0) for 5 min. Further digestion was stopped by adding an excess of soybean trypsin inhibitor (Sigma Chemical Co., St. Louis, MO). After the measurements, the disintegration of the axoneme without beating was observed by treating with 1 mM ATP to confirm the digestion of the axoneme.

Broken segments of the axoneme were obtained by homogenizing the demembranated flagella. Doublet microtubules were obtained by treating these segments for 90 s with 100 μ g/ml trypsin solution and then exposing to 1 mM ATP (cf. Summers

and Gibbons 1971).

The sperm suspensions were put into a trough (T in Fig.1) on the stage of a microscope for observation. One of the spermatozoa was fixed at its head of the tips of a braking micropipette (P) (cf. Hiramoto 1974) sucking the sperm head. The orientation of the spermatozoon was adjusted by tilting the micropipette attached to an instrument collar (I) held with a micromanipulator (M_1) (Ernst Leitz GmbH., Wetzlar, W. Germany) and rotating the micropipette about its axis so as to bring the entire length of the flagellum into the focal plane of the microscope. Since the micropipette was fixed to the instrument collar after passing through a hole set on the axis of the instrument collar, the spermatozoon at the tip of the micropipette was always in the microscopic field when the micropipette was rotated. A stream of the surrounding medium was generated by moving the trough at a constant speed controlled with an oil-pressure transmission mechanism of the micromanipulator (M_2 ; MO-102 Narishige Scientific Instrument Laboratory, Tokyo) holding the trough on the microscope stage. The direction of the x or y axis of the micromanipulator was adjusted beforehand to the x or y axis of the micromanipulator movement by rotating the stage to which the operating head of the micromanipulator was fixed. The speed of the medium was controlled with one of the two motors (D_1 and D_2), corresponding to x- or y- direction movement of the operating head, attached to the control unit of the micromanipulator. The flow speed of the medium in which the flagellum is

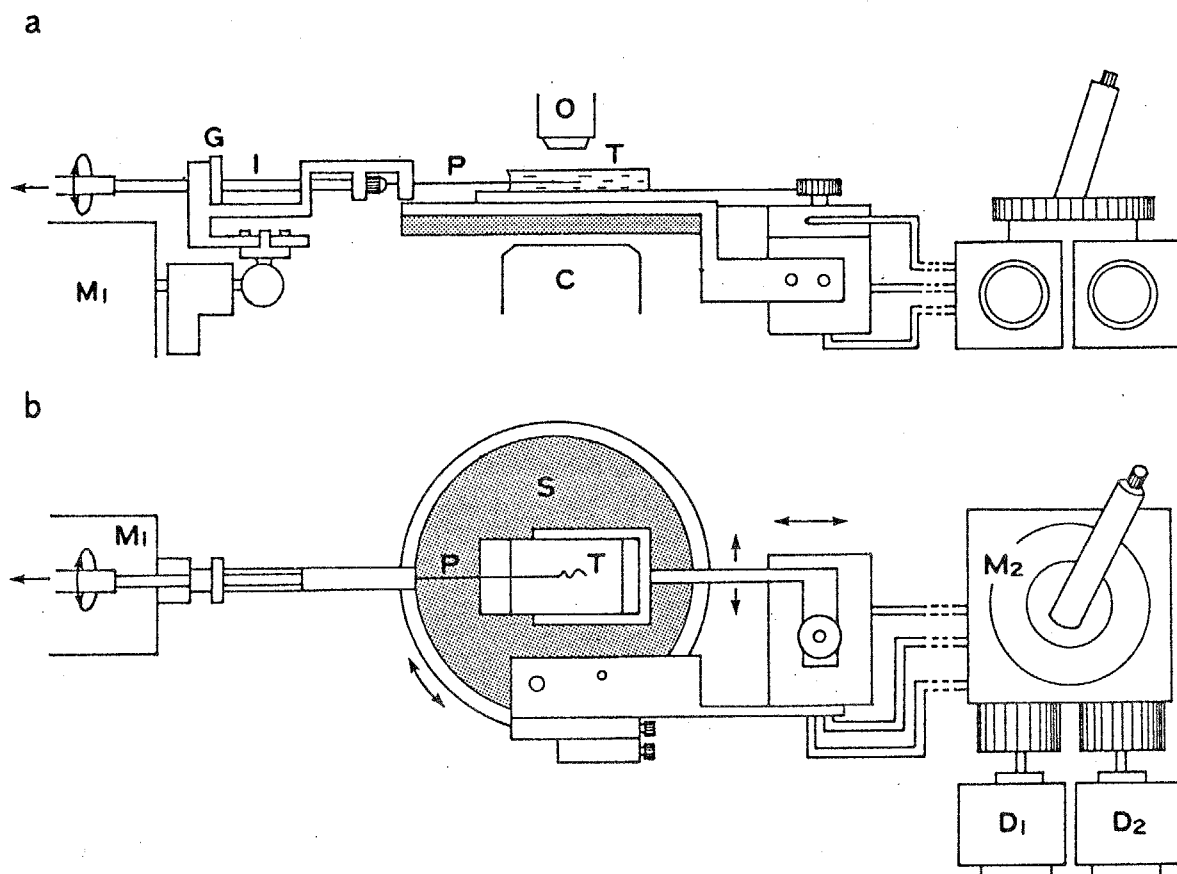


Fig.1. Experimental setup.

(a), front view; (b), plan view. C , long-focal-length condenser; D_1 and D_2 , motors; G , graduator measuring rotation angle of micropipette; I , instrument collar holding a micropipette; M_1 and M_2 , micromanipulators; O , objective lens; P , micropipette; S , microscope stage; T , trough.

exposed was determined from the speed of some particles occasionally located near the flagellum. In the case of flagella treated with Triton X-100, trypsin, EHNA, vanadate, the proximal region of the flagellum about 5 μ m from the base was sucked into the micropipette so as to support its base rigidly.

Observations of the flagella were made at a magnification 400 x with a Nikon phase contrast microscope with BM 40 x objective and a long-focal-length condenser. In the microscopic observation, a high-pressure mercury arc lamp (Model HH 100T Tiyoda Kogaku K.K., Tokyo) was used for illumination. In the photographic recording, the flagellum was illuminated with stroboscopic xenon flashes at the rate of 200 Hz (Model 100 Chadwick-Helmuth Co., Inc., Monrovia, CA) and then images of the flagellum formed with the microscope were recorded on Kodak Tri-X film moving at a constant speed, 1 m/s, after an appropriate magnification with the microscope lens system.

The procedure for recording the bending of doublet microtubules by the stream of the medium was as follows. A drop of the suspension of doublet microtubules prepared as mentioned above was put on a glass slide and covered with a coverslip keeping a definite distance with two strips of coverslip put in parallel with each other. The medium of doublet microtubules was made to flow by sucking the suspension at one end with a strip of dry filter paper applied to the other end. The flow speed was determined from the speed of some particles occasionally passing through

the vicinity of the doublet microtubules. Doublet microtubules which were attached to the coverslip at one end laying in the direction perpendicular to the flow were observed with a dark-field microscope with a Nikon dark-field condenser and an Olympus oil-immersion objective (HI Apo 40/1.00). Microtubules in a still medium and in moving medium were recorded on 16-mm Kodak 4 x negative film with a 16 mm cinecamera (H 16M, Bolex International S.A., Yverdon, Switzerland) at 4 frames per second at a magnification 100 x on the film by illuminating with a high-pressure mercury arc lamp.

Analysis of the photographic records of flagella was carried out by tracing the image of the flagellum on a sheet of paper after a 1500 x magnification with a photographic enlarger. Measurements were made directly with these traces.

The curvature of the bend in flagella was measured by finding a circle fitting to the trace of the bend among many template circles.

Effects of stationary stream of the medium on the flagellar movement

In flagellar movement of echinoderm spermatozoa, bending waves are initiated at the base of the flagellum and propagate toward the tip. Because the bending of the flagellum occurs in a definite plane, the image of the flagellum

which was in focus over its entire length could be observed as shown in Fig.2a by adjusting the beating plane to be perpendicular to the optimal axis of the microscope.

As shown in Fig.2b, when a stream was applied in the direction from the base to the tip of the flagellum, the wavelength increased and the amplitude decreased as if the waveform was stretched in the direction of the stream, and in consequence, the curvature of the bent portion of the flagellum decreased. When the speed of the stream increased, the curvature of the bend decreased and the wavelength increased, until finally, the waveform became irregular as shown in Fig.2d. When the speed of the stream was in the range from 300 to 400 $\mu\text{m/s}$, about two times the propulsive speed of freely swimming spermatozoa, new waves were never generated in the flagellum as shown in Fig.2e. When the speed of the stream exceeded 300-400 $\mu\text{m/s}$, the flagellum became almost straight without motility.

When a stream was applied in the direction from the tip to the base of the flagellum, the wavelength decreased and the amplitude increased as shown in Fig.2c. As the speed of the medium increased, the curvature of the bend increased, though the curvature of the bend of the flagellum did not exceed a definite value, $5 \times 10^{-3} \text{ cm}^{-1}$ (i.e. 2 μm in the radius of the curvature) as shown in Fig.2f. When the stream speed exceeded about 200 $\mu\text{m/s}$, the wave was distorted and became non-planar. Within the region about 5 μm from the base of the flagellum, the curvature of the bend of the flagellum was scarcely affected by

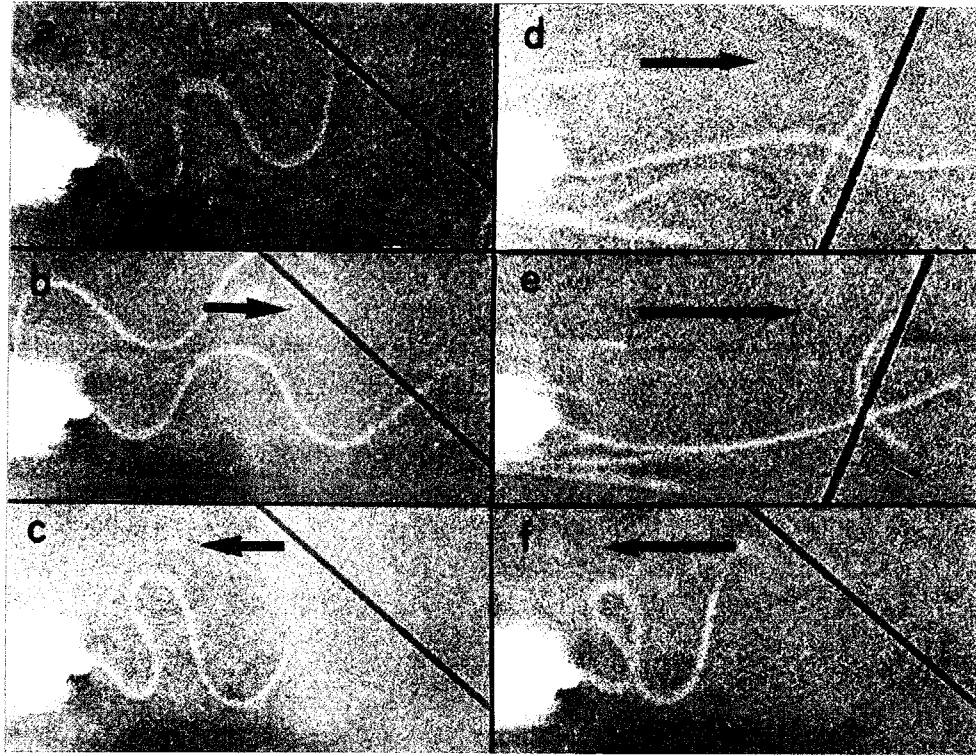


Fig.2. Changes in the form of the flagellum of a sand dollar spermatozoon by a stream of medium.

a, b, and c show the same spermatozoon. Arrows indicate the stream velocity.

the stream of the medium, suggesting that the flexural rigidity of the flagellum is larger in this regions than in remaining regions.

As shown in Fig.3, both the beat frequency and the number of waves contained in a flagellum were practically unchanged by the stream when the stream velocity was smaller than a definite value (280 $\mu\text{m/s}$ in the case of Fig.3), while both the beat frequency and the wave number decreased when the speed exceeded this value.

The effects of the stream of the medium on the waveform, the beat frequency and the wave number were reversible: They recovered to their original values when the stream of the medium was stopped.

When the micropipette holding the spermatozoon was rotated by 90° about its axis so as to bring the beating plane of the flagellum perpendicular to the field plane of the microscope, parts of the flagellum in focus were observed as a train of spots moving toward the tip of the flagellum as shown in Fig.4a-c. When the medium was moved in the direction perpendicular to the beating plane, the beating plane was bent by the stream as shown in Fig.4a'-c'. The degree of the bending of the beating plane depended on the speed of the stream. The parts of the flagellum observed in focus were continuously moving from the base of the flagellum toward the tip indicating the propagation of the bending wave, provided that the speed of the stream was smaller than 180 $\mu\text{m/s}$. In this case, the beat frequency was practically the same as normal beat frequency. When

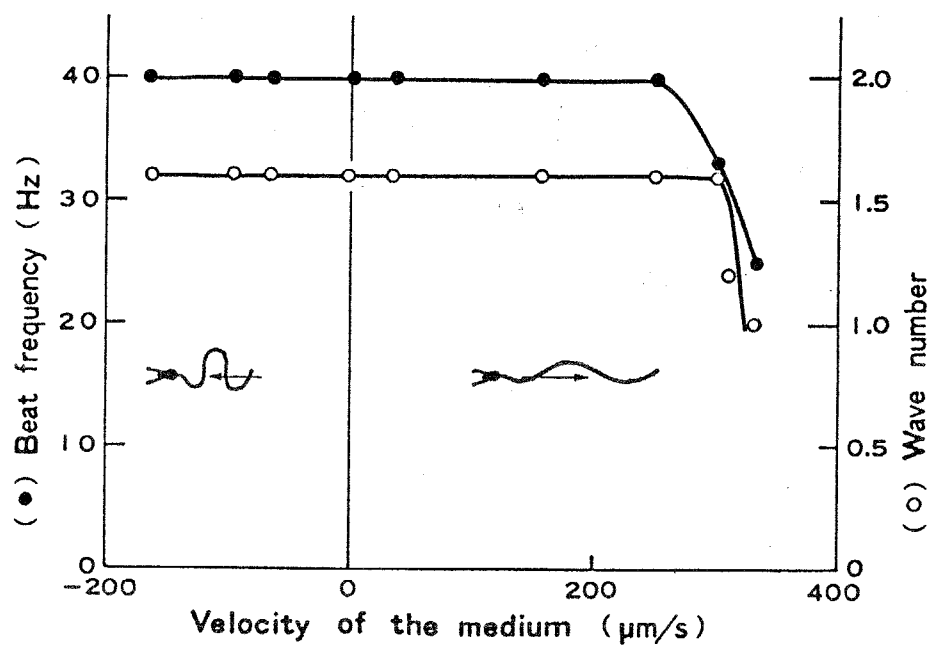


Fig.3. Changes in the beat frequency (●) and in the wave number (○) at various speed of the medium.

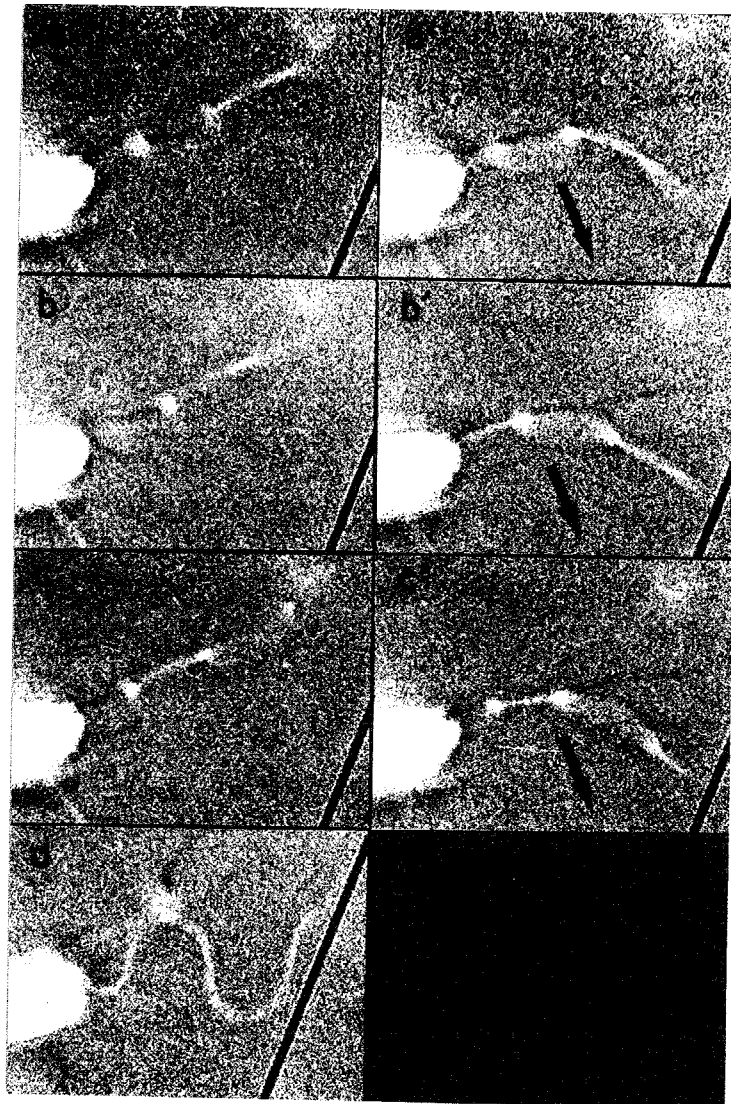


Fig.4. Bending of the beating plane of the flagellum of a sand dollar spermatozoon by the movement of the medium. a, b, and c are the same spermatozoon in various beating phase observed from the direction of the beating plane.

a', b', and c' show beating planes of the flagellum when the medium is moving in directions shown by arrows. d shows the form of the flagellum observed from the direction perpendicular to the beating plane.

the speed of the stream was larger than 180 $\mu\text{m/s}$, the flagellar beating deviated from the regular planar one. No difference in the degree of bending was found between stream of opposite directions provided that the absolute values of the stream speed were the same as shown in Figs.4a'-c'.

When demembranated flagella were put into the reactivating solution containing 1 mM ATP, they move in a manner similar to that of live flagella as reported by Gibbons and Gibbons (1972). Effects of stationary stream of reactivated demembranated flagella were similar to those of live flagella: The bending wave was "stretched" when the stream of medium was applied to the flagellum in the direction from the base to the tip of the flagellum and "compressed" when the stream direction was reversed; and the beating plane of the flagellum was bent when the stream was applied in the direction perpendicular to the beating plane.

Procedure for calculating flexural rigidity of flagella

In the present study, the bending stiffness of the flagellum without motion was determined from the relationship between the bending of the flagellum when its one end was fixed and the medium was moved at a definite speed and the bending moment due to the viscous resistance of the medium acting on the flagellum. In the same principle, the bending resistance was determined in demembranated

flagella (axonemes) and doublet microtubules.

The form of the flagellum beating in moving medium is different from the form of the same flagellum beating in still medium. The bending stiffness of the flagellum during beating was determined from the difference in the form of the flagellum beating in the moving medium from that of the flagellum beating in the still medium in the same beating phase and the viscous resistance of the medium expected to decrease when the movement of the medium is stopped, assuming that the above difference in the forms of the flagellum is due to the elastic deformation of the beating flagellum due to the difference in the movement of the medium. For satisfying this assumption, it is expected that the mechano-chemical processes generating the rhythmic beatings of the flagellum is not affected by the movement of the medium. It has been shown in the present experiment that the process determining the frequency of the beating is not affected provided that the speed of the medium is in the range smaller than $280 \mu\text{m/s}$ (cf. Fig.3), which was used in the present experiment.

The flexural rigidity of the flagellum was represented, for convenience, by the bending moment divided by the curvature of the flagellum i.e., the apparent flexural rigidity of the flagellum. If the flagellum were regarded as a homogeneous elastic body, the Young's modulus of the structural component of the flagellum would be determined by dividing the flexural rigidity by the second moment of the cross section of the flagellum. Because the flagellum is not regarded as a

homogeneous body, the present representation is merely for quantitative comparison of the bending stiffness among different conditions, e.g. the direction of the force application and chemical dissection component structures from flagellum.

A. The representation of the flagellar waveform by Fourier series

In the present study, the forms of beating flagella recorded by photographic means were simulated by Fourier series in order to facilitate calculations of viscous resistances and viscous bending moments acting on the flagellum.

In each tracing at a final magnification 1500 of the image of beating flagellum, an orthogonal coordinate system, O-XY was taken with the origin of the coordinate at base of the flagellum and the X-axis as the straight line connecting the base of the flagellum and the tip as shown in fig.5. The segment of the X axis between the origin and the tip X_t was divided into 12 equal-length portions and Y coordinates were measured for these 11 values of X coordinates. These Y coordinate values, Y_i ($i=1, 2, 3, \dots, 11$) were put in an electric calculator (41C Hewlett-Packard Co., Corvallis, OR) program which computed values of the Fourier coefficients a_k and b_k , by the following equations (Whittaker and Robinson 1926).

$$\left. \begin{aligned} a_k &= \begin{cases} \frac{1}{12} \sum_{i=1}^{11} Y_i & k=0 \\ \frac{1}{6} \sum_{i=1}^{11} Y_i \cos \frac{\pi}{6} i k & k=1, 2, 3, 4, 5 \\ \frac{1}{12} \sum_{i=1}^{11} Y_i \cos i \pi & k=6 \end{cases} \\ b_k &= \frac{1}{6} \sum_{i=1}^{11} Y_i \sin \frac{\pi}{6} i k \quad k=1, 2, 3, 4, 5 \end{aligned} \right\} (1)$$

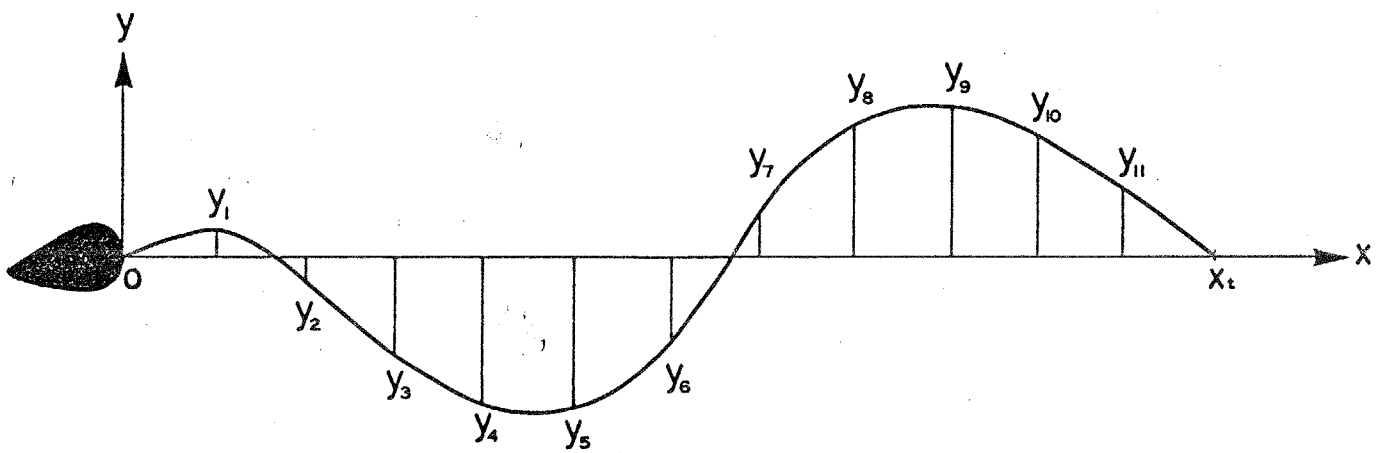


Fig.5. Fourier analysis of the flagellar waveform.

The waveform of the flagellum was represented by Fourier series of the form

$$Y = \sum_{k=0}^6 a_k \cos k\theta + \sum_{k=1}^5 b_k \sin k\theta, \quad \theta = 2\pi X / X_t. \quad (2)$$

and this representation was used in each of the following calculations.

B. Calculation of the flexural rigidity for the bending within the beating plane

The waveform of the beating flagellum fixed at its head changed by the viscous resistance of the medium acting on the flagellum when the medium was moved in parallel to the beating plane as shown in Fig.2.

Letting the equation simulating the waveform of the beating flagellum by Fourier series be $y=f(x)$ and letting the direction cosines of the tangent and normal at any point $Q(x, f(x))$ on the flagellum be \mathfrak{t} and \mathfrak{m} , respectively as shown in Fig.6, \mathfrak{t} and \mathfrak{m} are expressed as

$$\begin{aligned} \mathfrak{t} &= (1/\sqrt{1+\{f'(x)\}^2}, f'(x)/\sqrt{1+\{f'(x)\}^2}), \\ \mathfrak{m} &= (-f'(x)/\sqrt{1+\{f'(x)\}^2}, 1/\sqrt{1+\{f'(x)\}^2}). \end{aligned} \quad (3)$$

Position vector \mathbb{R} directed from point $P(x_p, f(x_p))$ to Q is expressed by

$$\mathbb{R} = (x - x_p, f(x) - f(x_p)). \quad (4)$$

The bending moment dM around point P due to the viscous resistances of the medium acting on a minute segment (length; ds) at point Q is given by

$$dM = df_L(\mathbb{R}, \mathfrak{m}) - df_N(\mathbb{R}, \mathfrak{t}), \quad (5)$$

where df_L and df_N are the components of the viscous resistance

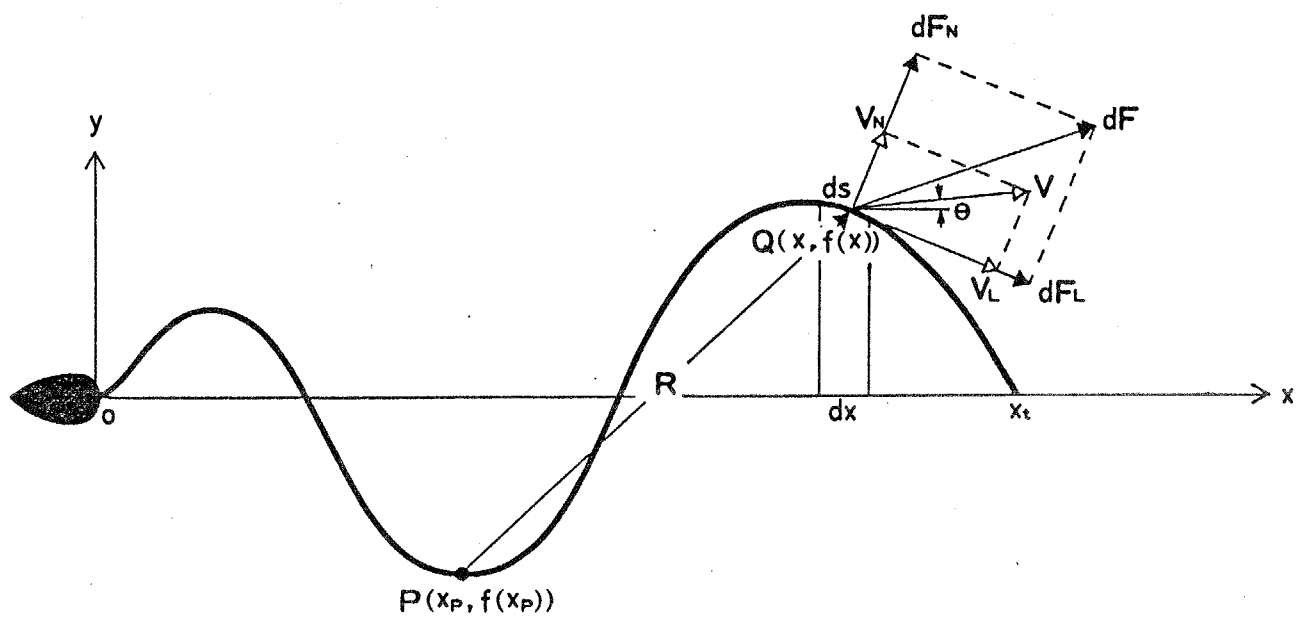


Fig.6. Diagram illustrating parameters in calculation of forces and bending moments.

(df) tangential and normal to the flagellar axis, respectively. According to Gray and Hancock (1955), the tangential and normal components, df_L and df_N , of the viscous resistance acting on the segment placed in a stream are given by

$$\begin{cases} df_L = (df, \hat{t}) = c_L v_L ds, \\ df_N = (df, \hat{n}) = c_N v_N ds. \end{cases} \quad (6)$$

where v_L and v_N are the velocity components tangential to and normal to the segment axis, respectively. c_L and c_N are coefficients of resistance for movement of the segment along to and normal the axis, respectively. According to Lighthill (1976), c_L and c_N for thin fibers such as flagella are given by

$$\begin{cases} c_L = 2\pi\mu / \ln(2q/a), \\ c_N = 4\pi\mu / [\ln(2q/a) + 0.5]. \end{cases} \quad (7)$$

where a is the radius of the flagellum, $q=0.09\Lambda$ (where Λ is the wavelength measured along the flagellum) and μ is the viscosity of the medium. In the present study, wavelength of the flagellar bending wave was in the range from 27 to 33 μm and viscosity of each working solution was 1.1×10^{-3} Pa.s for ASW and 2.5×10^{-3} Pa.s for both reactivating solution and the ATP-free medium as mentioned in Materials and Methods. Substituting these values and the radius of the flagellum $a=0.1 \mu\text{m}$ into (7) gives approximately constant values for c_L and c_N : $c_L=1.5 \times 10^{-3}$ Pa.s and $c_N=2.7 \times 10^{-3}$ Pa.s for ASW and $c_L=3.8 \times 10^{-3}$ Pa.s and $c_N=6.8 \times 10^{-3}$ Pa.s for both the reactivating solution and the ATP-free medium. These values were used for c_L and c_N in the present study.

Substituting (3), (4), and (6) into (5) and using $ds = \sqrt{1 + \{f'(x)\}^2} dx$ give the bending moment dM ,

$$dM = [C_L V_L \{(x_P - x)f'(x) + f(x) - f(x_P)\} - C_N V_N \{x - x_P + (f(x) - f(x_P))f'(x)\}] dx. \quad (8)$$

Expression of the components of the velocity, v_L and v_N , in terms of x component (v_x) and y component (v_y) of the velocity (v) can be written as:

$$v_L = (v_x + v_y f'(x)) / \sqrt{1 + \{f'(x)\}^2}, \quad v_N = (-v_x f'(x) + v_y) / \sqrt{1 + \{f'(x)\}^2}. \quad (9)$$

The total bending moment about the point P on the flagellum, where the curvature was determined, is the sum of the moments due to the resistances acting on all segments distal to that point. Substituting (9) into (8) and integrating the bending moment dM from the tip of the flagellum to P give total bending moment $M(x_P)$ around point $P(x_P, f(x_P))$ on the flagellum,

$$M(x_P) = \int_{x_T}^{x_P} dM = \int_{x_T}^{x_P} \frac{C_L \{v_x + v_y f'(x)\} \{(x_P - x)f'(x) + f(x) - f(x_P)\} - C_N \{-v_x f'(x) + v_y\} [x - x_P + \{f(x) - f(x_P)\} f'(x)]}{\sqrt{1 + \{f'(x)\}^2}} dx. \quad (10)$$

The calculation was made by loading the program of (10) into the electric calculator and inputting the data, the distance x_t from the base to the tip of the flagellum and both the speed v and the direction θ of the movement of the medium as shown in Fig.6.

In tracings at final magnification 1500, the curvature K of the bend at a point with maximum curvature and about 20 μm from the base (P in Fig.6) of flagellum beating in the moving medium and the curvature K_o of the bend of the same flagellum beating in the still medium in the same beating phase were measured as described in Materials and

Methods.

The flexural rigidity of the flagellum (S) was calculated by the following equation:

$$S = M(\alpha_P) / (\kappa - \kappa_0), \quad (//)$$

where $\kappa - \kappa_0$ is the difference of curvatures at point P between the flagellum beating in the moving medium and the flagellum in still medium as mentioned above.

C. Calculation of the flexural rigidity for the bending in the plane perpendicular to the beating plane

When the stream of the medium was applied in the direction perpendicular to the beating plane of the flagellum, the beating plane was bent by the stream as shown in Fig.4. The flexural rigidity for the bending in the plane perpendicular to the beating plane was determined by comparing the observed deformation with the deformation due to the bending and the twisting of the flagellum computed with the calculator using hydrodynamic theories and the waveform of the beating flagellum represented by Fourier series.

When flagellum is exposed to a stream of the medium flowing in the direction perpendicular to the beating plane, it is expected that the flagellum is bent and twisted by viscous resistances acting on the flagellum. In each tracing at final magnification 1500 of the image of the beating flagellum, the origin of coordinates O was taken at the base of the flagellum and the orthogonal coordinate system, O -xyz, with a straight line tangential to the

beating plane at the base of the flagellum and passing the tip as the x axis, the y axis in the beating plane and the z axis perpendicular to the x and y axes was taken as shown in Fig. 7.

Letting the equation simulating the waveform of the beating flagellum by Fourier series be $y=f(x)$ and letting the direction cosines of the tangent and the normal at point $Q(x_1, f(x_1))$ on the flagellum be θ_1 , ϕ_1 , respectively, θ_1 and ϕ_1 are expressed as

$$\begin{aligned}\theta_1 &= (1/\sqrt{1+\{f'(x_1)\}^2}, f'(x_1)/\sqrt{1+\{f'(x_1)\}^2}), \\ \phi_1 &= (-f'(x_1)/\sqrt{1+\{f'(x_1)\}^2}, 1/\sqrt{1+\{f'(x_1)\}^2}).\end{aligned}\quad (12)$$

Position vector R_1 directed from a point Q on the flagellum to the tip and position vector R_2 directed from point Q to $R(x_2, f(x_2))$ between Q and the tip of the flagellum, are written as:

$$\begin{aligned}R_1 &= (x_2 - x_1, -f(x_1)) , \\ R_2 &= (x_2 - x_1, f(x_2) - f(x_1)) .\end{aligned}\quad (13)$$

If the speed of the medium is represented by v , the viscous resistance $c_N v$ per unit length acts on each part of the flagellum (Gray and Hancock 1955). The bending moment dM around point Q on the flagellum due to the viscous resistance of the medium acting in a minute segment (length: ds_2) at point R is given by

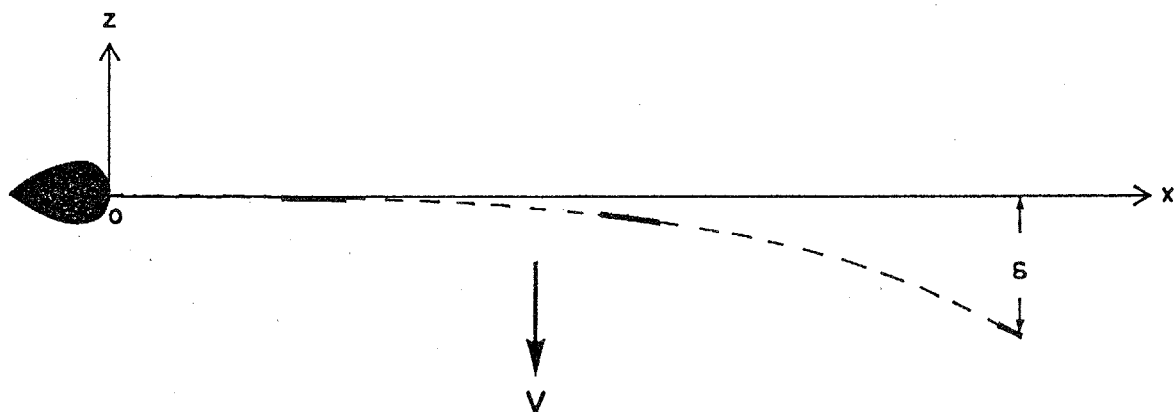
$$dM = c_N v (R_2, \theta_1) ds_2 . \quad (14)$$

Substituting (12) and (13) into (14) and using $ds_2 = \sqrt{1+\{f'(x_2)\}^2} dx_2$ give the bending moment dM ,

$$dM = c_N v \frac{x_2 - x_1 + \{f(x_2) - f(x_1)\} f'(x_1)}{\sqrt{1+\{f'(x_1)\}^2}} \cdot \sqrt{1+\{f'(x_2)\}^2} dx_2 . \quad (15)$$

Integrating the bending moment dM from the tip of the flagellum

a



b

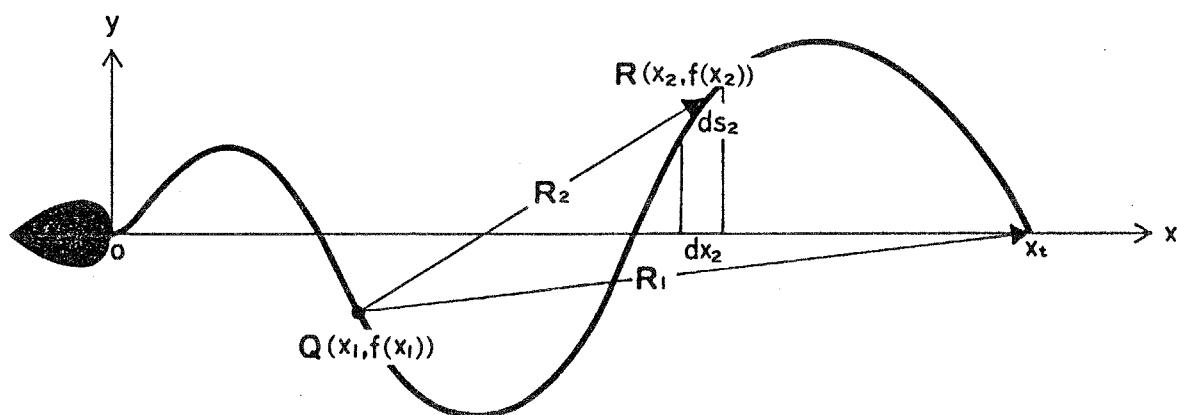


Fig.7. Diagram illustrating parameters in calculation of the flexural rigidity for bending in the plane perpendicular to the beatibg plane.

to Q gives total bending moment $M(x_1)$ around point Q,

$$M(x_1) = C_N \nu \int_{x_1}^{x_2} \frac{(x_2 - x_1) + \{f(x_2) - f(x_1)\}f'(x_1)}{\sqrt{1 + \{f'(x_1)\}^2}} \cdot \sqrt{1 + \{f'(x_2)\}^2} dx_2. \quad (16)$$

The total bending moment $M(x_1)$ is proportional to the slope $\theta_M(x_1)$ of the flagellum at point Q due to the bending of the flagellum.

$$\theta_M(x_1) = M(x_1) / S. \quad (17)$$

where S is the flexural rigidity.

The deflection at the tip of the flagellum due to the bending of the all segments is obtained by integrating of deflections due to all segments from the base to the tip of the flagellum:

$$\delta_B = \int_0^{x_1} (R_1, \theta_1) \cdot \theta_M(x_1) \sqrt{1 + \{f'(x_1)\}^2} dx_1. \quad (18)$$

The torsional moment dT around point Q due to the viscous resistances of the medium acting on a segment (length: ds_2) at point R is given by

$$dT = C_N \nu (R_2, \theta_2) ds_2. \quad (19)$$

Substituting (12) and (13) into (19) and using $ds_2 = \sqrt{1 + \{f'(x_2)\}^2} dx_2$ give the torsional moment dT,

$$dT = C_N \nu \frac{(x_1 - x_2)f'(x_1) + f(x_2) - f(x_1)}{\sqrt{1 + \{f'(x_1)\}^2}} \cdot \sqrt{1 + \{f'(x_2)\}^2} dx_2. \quad (20)$$

Integrating the torsional moment dT from the tip of the flagellum to Q gives total torsional moment $T(x_1)$ around point Q on the flagellum,

$$T(x_1) = C_N \nu \int_{x_1}^{x_2} \frac{(x_1 - x_2)f'(x_1) + f(x_2) - f(x_1)}{\sqrt{1 + \{f'(x_1)\}^2}} \cdot \sqrt{1 + \{f'(x_2)\}^2} dx_2. \quad (21)$$

The total torsional moment $T(x_1)$ is proportional to the angle of twist per unit length $\theta_T(x_1)$.

$$\theta_T(x_1) = T(x_1) / C. \quad (22)$$

where C is the torsional rigidity.

The deflection (δ_T) at the tip of the flagellum

due to the torsion of all segments is obtained by integrating of deformation due to elementary segments from the base to the tip of the flagellum:

$$\delta_T = \int_0^{x_t} (R_1, M_1) \cdot \theta_T(x_1) \sqrt{1 + \{f'(x_1)\}^2} dx_1. \quad (23)$$

If it is assumed that the flagellum is regarded as a uniform elastic rod with a circular cross section and that the Poisson's ratio is 0.5, the flexural rigidity (S) is 1.5 times the torsional rigidity (C) according to elementary theories of elasticity.

Adding the deflection due to the bending and the deflection due to the torsion, and using $S=1.5C$, total deflections (δ) is given by

$$\delta = \frac{C \omega V}{S} \left[\int_0^{x_t} \int_{x_1}^{x_2} \frac{\{x_t - x_1 - f(x_1) f'(x_1)\} \{x_2 - x_1 + (f(x_2) - f(x_1)) f'(x_1)\}}{\sqrt{1 + \{f'(x_1)\}^2}} \cdot \sqrt{1 + \{f'(x_2)\}^2} dx_1 dx_2 \right. \\ \left. + 1.5 \int_0^{x_t} \int_{x_1}^{x_2} \frac{\{(x_1 - x_2) f'(x_1) - f(x_1)\} \{(x_1 - x_2) f'(x_2) + f(x_2) - f(x_1)\}}{\sqrt{1 + \{f'(x_1)\}^2}} \cdot \sqrt{1 + \{f'(x_2)\}^2} dx_1 dx_2 \right]. \quad (24)$$

Total deflections at the tip of the flagellum was obtained by loading the program of equation (24) into the electric calculator and inputting the data, the distance x_t from the base to the tip and the speed v of the stream of the medium, measured on the tracings of the beating flagellum.

D. Calculation of the flexural rigidity of motionless flagella

When a stream of the medium was applied in the direction perpendicular to the tangent at the base of the flagellum, the flagellum of spermatozoon fixed at its head to the tip of a micropipette was bent by the viscous resistance of the medium acting on the flagellum as shown in Fig.8.

The deflection y of the flagellum at the tip by the

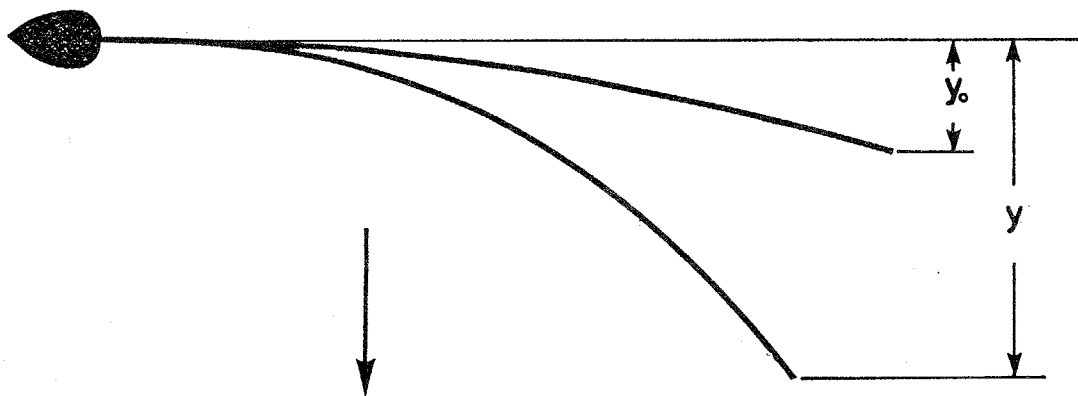


Fig.8. The deformation of the motionless flagellum of a sand dollar spermatozoon when a stream was applied in the direction at right angles to the tangent at the base of the flagellum. Arrows indicate the stream direction.

viscous drags of the medium acting on all segments along the flagellum was calculated numerically for various values of flexural rigidity, assuming that the flagellum is approximated to a series of circular arcs tangent to one another at their points of intersections (cf. Seames and Conway 1957). Values of drag coefficient c_N mentioned above, 2.7×10^{-3} pa.s for ASW and 6.8×10^{-3} pa.s for reactivating solution and the ATP-free medium were used in the present calculation. The flexural rigidity of motionless flagella was obtained by finding the value for flexural rigidity in which the calculated and observed deflections at the tip of the flagellum.

E. Calculation of the flexural rigidity of doublet microtubules

The principle of calculation of the flexural rigidity of doublet microtubules was the same as that of motionless flagella. Doublet microtubules attached to a coverslip at the proximal region bent by the viscous resistance of the medium, when a stream of medium was applied in the direction to the tangent at the base of doublet microtubules. The flexural rigidity of doublet microtubules was calculated from the bend by the stream and the viscous resistance caused by the stream. The coefficient of viscous resistance corrected for effects of the coverslip was calculated from equation,

$$c_N = 4\pi\mu / \ln(2h/r),$$

where h is the distance of the microtubule from the coverslip, r is the radius of the microtubule and μ is the viscosity

of the medium, according to Katz and Blake (1975). In the present study, the value 4.6×10^{-2} Pa.s was used for c_N , which was obtained by substituting the values, $h=25$ nm, $r=25$ nm, and $\mu=2.5 \times 10^{-3}$ Pa.s, into (25).

Flexural rigidity of sea urchin sperm flagella

A. Flexural rigidity of beating flagella

The average flexural rigidity of flagella of Clypeaster japonicus beating in the ASW was 4.2×10^{-22} Nm² determined at points about 20 μ m from the base (cf. Table I). The average flexural rigidity of Pseudocentrotus depressus flagella was 4.6×10^{-22} Nm², which was similar to that of Clypeaster japonicus. No significant difference was found in the flexural rigidity between measurements using the stream from the base to the tip of the flagellum "stretching" the flagellar wave and the stream from the tip to the base of the flagellum "compressing" the flagellar wave.

The average flexural rigidity of beating flagella of Clypeaster japonicus for bending in the plane perpendicular to the beating plane was 5.8×10^{-21} Nm², 14 times that of beating flagella for bending within the beating plane (see Table I). In Pseudocentrotus depressus, the average flexural rigidity for bending in the plane perpendicular to the beating plane was 7.1×10^{-21} Nm², 15 times that

Table I. Flexural rigidity of sea urchin sperm flagella (10^{-21} Nm²).

		(mean)			
		Motionless		Beating	
		Medium		Medium	
				a ¹⁾	b ²⁾
Living flagella	CO ₂ -saturated S.W.	11 ± 6	Normal S.W.	0.42 ± 0.31	5.8 ± 2.6
	2 mM EHNA, A.S.W.	0.19 ± 0.04			
Demembranated flagella	0 mM ATP	14 ± 4	1 mM ATP	1.0 ± 0.6	12 ± 3
	2 μM ATP	15 ± 8			
	1 mM ATP, 10 μM vanadate	0.31 ± 0.15			
	1 mM ATP, 2 mM EHNA	0.28 ± 0.09			
Trypsin-digested demembranated flagella	0 mM ATP	16 ± 5			
Doublet microtubules	0 mM ATP	0.06 - 0.23			
	0.1 mM ATP	0.01 - 0.38			

1) Bending in the beating plane.

2) Bending in the direction perpendicular to the beating plane.

for bending within the beating plane mentioned above.

B. The flexural rigidity of motionless living flagella

As shown in Fig.9, the flagellum of spermatozoon fixed at its head to the tip of a micropipette was bent by the viscous resistance of the medium acting on the flagellum when a stream of the medium was applied in the direction perpendicular to the tangent at the base of the flagellum.

In spermatozoa which had lost their motility in CO_2 -ASW, the flagellum was slightly curved and its head was often tilted to the concave side of the flagellum. When the spermatozoa were transferred to normal ASW, they swam along circular paths keeping the convex sides of the flagella to the centers of the circles as reported by Goldstein (1979).

In Clypeaster japonicus, the average flexural rigidity of living flagella immobilized in CO_2 -ASW was $1.1 \times 10^{-20} \text{ Nm}^2$ when tested by bending within the beating plane

(cf. Table I). In Pseudocentrotus depressus, a similar value ($1.3 \times 10^{-20} \text{ Nm}^2$) was obtained (cf. Table I). It was very difficult to bend the flagellum in the direction perpendicular to the "beating" plane, the plane in which the flagellum is expected to beat when the flagellum resumed moving, because the flagellum was twisted in many cases.

In one case where the flagellum could be bent in the perpendicular plane, no difference in the flexural rigidity was found in the flexural rigidity from the flexural rigidity determined

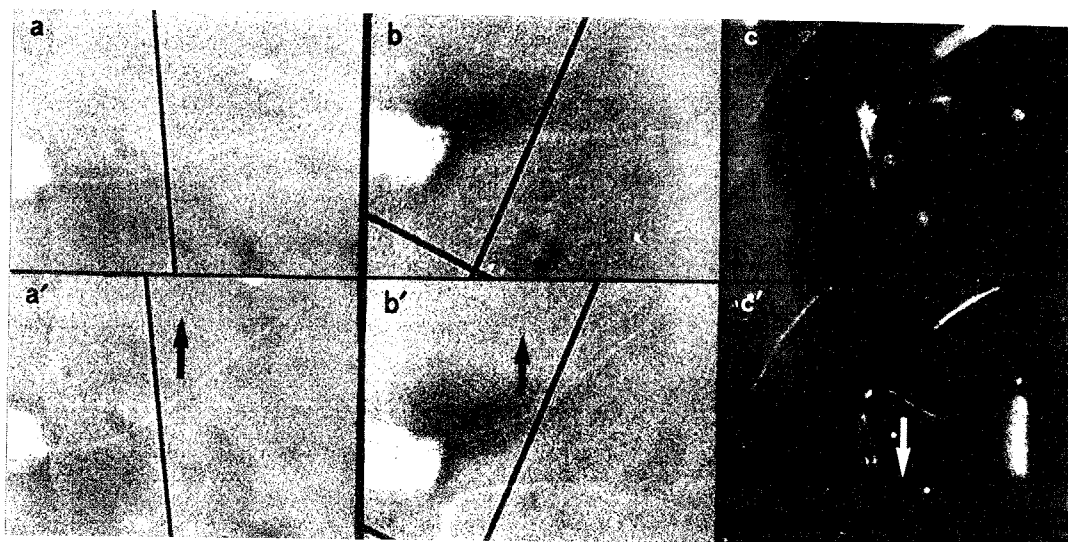


Fig.9. Changes in the form of the flagellum (a, a', b, and b') and doublet microtubules (c and c') of a sand dollar spermatozoon by stream of the medium. a, b, and c are in still medium and a', b', and c' are in the medium moving in the direction indicated by arrows.

by bending the flagellum in the "beating" plane.

C. The flexural rigidity of demembranated flagella reactivated with ATP

As shown in Table I, the average flexural rigidity of reactivated demembranated flagella was $1.0 \times 10^{-21} \text{ Nm}^2$ in Clypeaster japonicus and $6.1 \times 10^{-22} \text{ Nm}^2$ in Pseudocentrotus depressus. No difference was found between the flexural rigidity determined by "stretching" the flagellar wave by stream flowing from the base to the tip of the flagellum and that determined by "compressing" by the stream in opposite direction.

As shown in Table I, the average flexural rigidity of reactivated demembranated flagella for bending in the plane perpendicular to the beating plane was $1.2 \times 10^{-20} \text{ Nm}^2$, 12 times that of reactivated flagella for bending within the beating plane in Clypeaster japonicus and $1.0 \times 10^{-20} \text{ Nm}^2$, 17 times that of beating flagella for bending within the beating plane in Pseudocentrotus depressus.

It is noted that the values of flexural rigidity in reactivated demembranated flagella are similar to those in intact beating flagella.

D. The flexural rigidity of motionless demembranated flagella

The flexural rigidity of demembranated flagella obtained by treating normal flagella with Triton X-100 was measured

in ATP-free medium and in medium containing 2 μM ATP.

The average flexural rigidity of motionless demembranated flagella was $1.4 \times 10^{-20} \text{ Nm}^2$ in ATP-free medium and $1.5 \times 10^{-20} \text{ Nm}^2$ in medium containing 2 μM ATP in Clypeaster japonicus (cf. Table I).

E. Effects of vanadate on the flexural rigidity of demembranated flagella

Demembranated spermatozoa beating in reactivating solution containing 1 mM ATP were put into solutions containing various amounts of sodium vanadate and 1 mM ATP. In the presence of vanadate, up to 2 μM , the beat frequency reduced, while other parameters were scarcely changed. When the vanadate concentration exceeded 2 μM , some nonmotile spermatozoa were noticed. The sperm flagella, which were immobilized by 3 to 4 μM vanadate, were slightly curved along their length and rather straight in solutions containing 5 μM or more vanadate.

The average flexural rigidity of motionless demembranated flagella in the medium containing 1 mM ATP and 10 μM vanadate was $3.1 \times 10^{-22} \text{ Nm}^2$, which is only 2 per cent of that of motionless demembranated flagella in ATP-free medium and similar to that of beating flagella for bending within the beating plane (cf. Table I). No difference in flexural rigidity was found for the measurements carried out by bending in one plane and bending in the perpendicular to the former.

F. Effects of EHNA on the flexural rigidity of flagella

Spermatozoa beating in ASW were put into solutions containing various concentrations of EHNA. EHNA caused no change in flagellar movement, when the concentration was less than 0.5 mM. However, when concentrations of EHNA exceeded 0.5 mM, a few nonmotile spermatozoa were noticed in the sample, and fifty per cent of spermatozoa became immotile by 2 mM EHNA. The average flexural rigidity of motionless living flagella poisoned with 2 mM was $1.9 \times 10^{-22} \text{ Nm}^2$ (cf. Table I).

Demembranated spermatozoa beating in reactivating solution containing 1 mM ATP were put into solutions containing various concentrations of EHNA and 1 mM ATP. Effects of EHNA on demembranated flagella were similar to that of EHNA on living flagella: EHNA, up to 0.5 mM, caused no effect on flagellar movement. As the EHNA concentration increased, beat frequency of flagella decreased, and other wave parameters were little or no changed. Fifty per cent inhibition in the sample was obtained by 2 mM EHNA.

The average flexural rigidity of motionless demembranated flagella in the medium containing 1 mM ATP and 2 mM EHNA was $2.8 \times 10^{-22} \text{ Nm}^2$, similar to that of motionless demembranated flagella in the medium containing 10 μM sodium orthovanadate.

G. The flexural rigidity of trypsin-digested demembranated flagella

The demembranated flagella which had been treated with a solution containing 100 µg/ml trypsin for 5 min were fixed by sucking the proximal region of the flagellum into a micropipette was bent when a stream of the medium was applied as mentioned above. The average flexural rigidity of flagella demembranated with trypsin in ATP-free solution was $1.6 \times 10^{-20} \text{ Nm}^2$, which was similar to that of living flagella immobilized in CO_2 -ASW (cf. Table I).

H. The flexural rigidity of doublet microtubules

Doublet microtubules were obtained by treating trypsin-treated demembranated flagella with 1 mM ATP. As shown in Figs. 9c and c', doublet microtubules attached to the coverslip at one end were bent when a stream of medium was applied in the direction perpendicular to the tangent at attached end of the microtubules. The flexural rigidity of doublet microtubules was $6.1\text{--}23 \times 10^{-23} \text{ Nm}^2$ in ATP-free medium and $1.4\text{--}38 \times 10^{-23} \text{ Nm}^2$ in a medium containing 0.1 mM ATP (cf. Table I).

Discussion

As shown in Fig. 3, both the beat frequency and the

wave number were practically unchanged by the stream when the speed was smaller than a definite value (280 $\mu\text{m/s}$ in the case of Fig.3). As reported by Gibbons and Gibbons (1973), beat frequency is directly proportional to the number of dynein arms which are responsible for generating the sliding movements between doublet microtubules that induce propagated bending movements in intact sperm. Therefore, it seems likely that the process of active force generation in beating flagella is not affected by the stream of the medium within the above range.

The flexural rigidity of flagella determined in the present study are similar to those of demembranated flagella in ATP-free medium ($1.1 \times 10^{-20} \text{ Nm}^2$ for Hemicentrotus pulcherrimus) obtained by Okuno and Hiramoto (1979) and those in the medium containing 10 μM vanadate and 1 mM ATP ($8.9 \times 10^{-22} \text{ Nm}^2$ for Lytechinus pictus) obtained by Okuno (1980). However, in living flagella immobilized in CO_2 -ASW, the flexural rigidity in the present study ($1.1 \times 10^{-20} \text{ Nm}^2$) is larger than that obtained by Okuno and Hiramoto (1979) ($0.3\text{--}1.5 \times 10^{-21} \text{ Nm}^2$).

According to Brokaw and Simonic (1976) and Brokaw (1977), CO_2 causes direct inhibition of bend angle without affecting frequency, while the change in ATP concentration causes large changes in the beat frequency and little change in wavelength and amplitude of the bending waves. They also showed that spermatozoa stop motion suddenly and retain "rigor wave" configuration, when suddenly exposed to a relatively high CO_2 concentration, similarly to those obtained

by a sudden reduction in ATP concentration as reported by Gibbons and Gibbons (1974), while the spermatozoa slow down their movement and eventually stop showing nearly straight configurations at low CO₂ concentrations. Because the spermatozoa were suddenly put into CO₂-ASW containing a high CO₂ concentration in the present study, it is possible that the spermatozoa was in "rigor" state, and in consequence, has a high stiffness.

It is noted in Table I that values of the flexural rigidity of demembranated flagella in ATP-free medium and that in the medium containing 2 μ M ATP are more or less the same as those in living flagella immobilized with CO₂-ASW. This fact suggests that the cell membrane has a minor contribution to the rigidity of the flagellum. It is also noted that the flexural rigidity of demembranated flagella is scarcely affected by digestion with trypsin removing radial spokes and nexin links. This fact suggests that spokes and nexin links have minor contributions to the flexural rigidity of the axoneme. Gibbons and Gibbons (1974) reported that digestion of rigor wave of the axoneme with trypsin to an extent sufficient to destroy most of the spokes and nexin links has no effect on the form of the rigor wave.

As reported by Okuno and Hiramoto (1979), the stiffness of demembranated flagella is decreased by addition of ATP to the solution and become equivalent to that of live ones in the medium containing 10 mM ATP. As mentioned above, the flexural rigidity of motionless flagella immobilized

with EHNA and vanadate, which inhibit dynein ATPase activity, was only several per cent of that of motionless demembranated flagella in ATP-free medium (see Table I). According to Okuno (1980), the flagellum is in a relaxed state in the presence of MgATP^{2-} and vanadate. These results suggest that the flexural rigidity of the flagellum is mainly due to the axoneme structure consisting of microtubules connected with dynein arms.

As shown in Table I, the flexural rigidity for the bending with the beating plane is far smaller than that for the bending in the plane perpendicular to the beating plane in living beating flagella. Similar results were obtained in demembranated flagella reactivated with ATP. In both cases, the flagellum is flexible more than ten times for the bending within the beating plane compared with that for the bending in the perpendicular plane.

Values of the flexural rigidity in beating demembranated flagella determined by bending in the direction perpendicular to the beating plane were more or less the same as those in living motionless flagella in CO_2 -ASW, demembranated flagella in ATP-free or $2\mu\text{M}$ ATP medium, and trypsin-digested demembranated flagella. The flexural rigidity of beating flagella for the bending within the beating plane was similar to those of motionless flagella immobilized with EHNA or vanadate. This fact suggests that the active sliding between doublet microtubules responsible for the flagellar movement reduces the flexural rigidity of the flagellum for the bending in the beating plane, while in the direction

perpendicular to the beating plane, the active sliding between doublet microtubules does not seem to occur, consequently, there is no reduction of the flexural rigidity.

This remarkable difference in the flexural rigidity may be due to the difference in the number of dynein arms connecting adjacent doublet microtubules in different doublet couples: The number of dynein arms projecting in the direction at right angles to the beating plane is larger than that of arms projecting in parallel to the beating plane.

Flexural rigidity of doublet microtubules obtained by disintegrating the trypsin-treated demembranated flagella with ATP was determined from their bending by the stream of the surrounding medium. The wide variation of the rigidity values shown in Table I may be due to variation of the number of doublet microtubules contained in fibers used in experiment. Minimum values in the Table ($6.1 \times 10^{-23} \text{ Nm}^2$ in ATP-free medium and $1.4 \times 10^{-23} \text{ Nm}^2$ in medium containing 0.1 mM ATP) may indicate the rigidity of single doublet microtubules.

The Young's modulus of the doublet microtubule is calculated from its flexural rigidity and the second moment of its cross section. The latter is calculated to be $3.8 \times 10^{-32} \text{ m}^4$, if it is assumed that both A- and B-tubule have elliptical cross section with 5 nm wall thickness and the outer diameter of the cross section of the A-tubule is 25 nm in major axis and 23 nm in minor axis and the outer diameter of the cross section of the B-tubule is 29 nm in major axis and 22 nm in minor axis. Young's

modulus of microtubules is estimated to be 3.7×10^8 Pa from the lowest values of the flexural rigidity of doublet microtubule in the present study (1.4×10^{-23} Nm²). This value for Young's modulus is reasonable for a protein fiber: e.g. Young's modulus for flagellin of bacterial flagella (Fujime et.al 1972) is 10^{10} Pa, the order of 10^{10} Pa for F-actin of striated muscles (Oosawa 1980), the order of 10^9 Pa for collagen (Mason 1965), the order of 10^8 Pa for DNA (Cohen and Eisenberg 1966), and the order of 10^8 - 10^{10} Pa for silk (Wainwright et.al 1982).

Summary

1. The stiffness (flexural rigidity) of sea urchin sperm flagella was determined from their deformation when a stream of medium was applied and the bending moment acting on the flagella caused by the viscous resistance of medium.
2. The flexural rigidity of the flagellum beating in normal sea water was 5.8×10^{-21} Nm² for bending in the direction perpendicular to the beating plane and was 4.2×10^{-22} Nm² for bending within the beating plane.
3. A similar difference in the flexural rigidity by the difference in bending directions was found in demembranated flagella reactivated with 1 mM ATP: The flexural rigidity was 1.2×10^{-20} Nm² for bending in the direction perpendicular to the beating plane and 1.0×10^{-21} Nm² for bending within

the beating plane.

4. The flexural rigidity of living flagella immobilized in CO₂-saturated sea water was $1.1 \times 10^{-20} \text{ Nm}^2$.
5. The flexural rigidity of motionless demembranated flagella was $1.4 \times 10^{-20} \text{ Nm}^2$ in ATP-free medium and was $1.5 \times 10^{-20} \text{ Nm}^2$ in medium containing $2 \mu\text{M}$ ATP.
6. The flexural rigidity of motionless flagella in medium containing 1 mM ATP and $10 \mu\text{M}$ vanadate which inhibits dynein ATPase activity was $3.1 \times 10^{-22} \text{ Nm}^2$, which is only 2 per cent of that of motionless demembranated flagella in ATP-free medium and similar to that of beating flagella for the bending within the beating plane.
7. The flexural rigidity of motionless living flagella poisoned with 2 mM erythro-9-[3-(2-(Hydroxynonyl)) adenine [EHNA] which inhibits dynein ATPase was $1.9 \times 10^{-22} \text{ Nm}^2$.
8. The flexural rigidity of motionless demembranated flagella in medium containing 1 mM ATP and 2 mM EHNA was $2.8 \times 10^{-22} \text{ Nm}^2$.
9. The flexural rigidity of demembranated flagella digested with trypsin in ATP-free medium was $1.6 \times 10^{-20} \text{ Nm}^2$.
10. The flexural rigidity of doublet microtubules obtained by disintegrating trypsin-treated demembranated flagella with 1 mM ATP was $6.1-23 \times 10^{-23} \text{ Nm}^2$ in ATP-free medium and $1.4-38 \times 10^{-23} \text{ Nm}^2$ in medium containing 0.1 mM ATP.
11. These results suggest that the flexural rigidity of the flagellum is mainly due to axonemal structure consisting of outer doublet microtubules connected with dynein cross-

bridges, while the cell membrane, spokes and nexin links scarcely contribute to the flexural rigidity of the flagellum.

It is inferred that the difference in the flexural rigidity of beating flagella by the difference in bending direction is due to the difference of the number of dynein cross-bridges formed between different couples of adjacent doublet microtubules.

FLEXURAL RIGIDITY OF MAMMALIAN SPERM FLAGELLA

Introduction

Rodent sperm flagellum is one of the unique materials in studies of flagellar movement. The spermatozoan has a hook-shaped head (Fig.1a). The axoneme is surrounded by nine outer coarse fibers, forming a 9+9+2 cross sectional pattern (Fig.1b). Bending waves are initiated at the base of the flagellum and propagated toward the tip and the beating plane is almost planer. Judging from the analogy with mouse and rat spermatozoa, the directionality of the axoneme structure is known from the direction of the hook-shaped sperm head observed by light microscopy (Wooley 1977). From an analysis of waveforms of golden hamster spermatozoa fixed by rapid freezing, Woolley (1977) concluded that the principal bend, which is more effective and persists for a longer period than the reverse bend during flagellar beat cycle, occurs in the direction in which the head projection points, and that the convex edge of the principal bend contains doublet microtubule No.1 and the convex edge of the reverse bend contains doublet Nos.5 and 6 (Fig.1a).

Lindemann, Rudd and Rikmenspoel (1973) determined the flexural rigidity of motionless bull sperm flagella from the rate of recoil of the flagellum from passive bending with a microscope. They obtained values of $5 \times 10^{-20} \text{ Nm}^2$ and $4 \times 10^{-21} \text{ Nm}^2$ in the absence of ATP and in the presence of 10 mM ATP, respectively. This fact shows

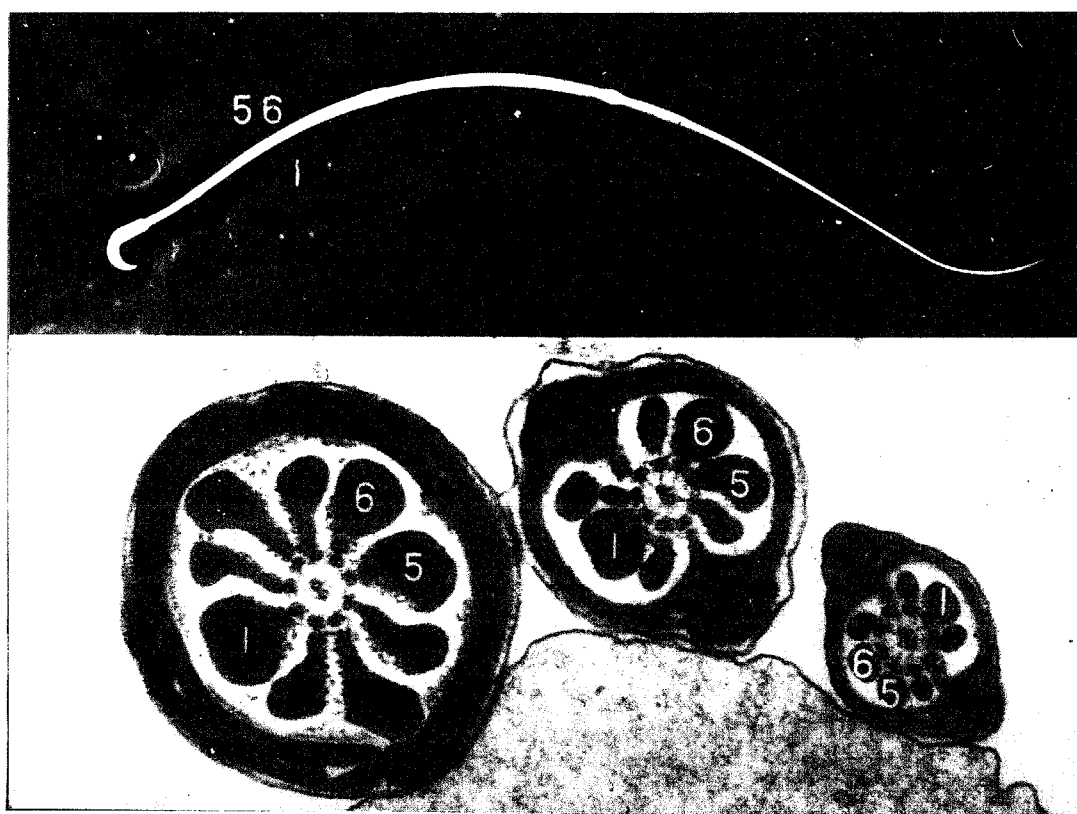


Fig.1. The structure of the golden hamster spermatozoon.

(a) Differential interference micrograph.

(b) Electron micrograph of the cross section of flagella.

that the stiffness is reduced by the presence of ATP.

In the present study, the flexibility of the mammalian sperm flagella in golden hamster spermatozoa was examined by the method described in CHAPTER I: A stationary stream of the medium of various directions was applied to the spermatozoon fixed at its head to the tip of a sucking micropipette and the relation between the change in the form of the flagellum and the viscous resistance of the medium acting on the flagellum was determined.

Material and Methods

The cauda epididymis of the golden hamster Mesocricetus auratus placed in Tyrode's solution (0.137 M NaCl, 2.7 mM KCl, 1.8 mM $\text{CaCl}_2 \cdot 2\text{H}_2\text{O}$, 0.49 mM $\text{MgCl}_2 \cdot 6\text{H}_2\text{O}$, 0.36 mM $\text{NaH}_2\text{PO}_4 \cdot 2\text{H}_2\text{O}$, 5.56 mM Glucose, 11.9 mM NaHCO_3 , pH 7.4) was minced with fine scissors. The extruded sperm suspension was filtered through a double layer of tissue paper (Kimwipes, Kimberly-Clark) and centrifuged at 4000 rpm for 5min. The sediment of 1 μl was resuspended in 10 ml of Tyrode's solution. In some experiments, the sperm flagella in the Tyrode's solution containing 10 mM sodium azide (Yoneyama Yakuhin Kogyo Co., Ltd. Oosaka) (cf. Mohri 1956) were used.

To prepare demembranated sperm flagella, 5 μl of the sedimented sperm suspension was added to 0.2 ml of extracting solution (0.1% v/v Triton X-100, 0.2 M sucrose, 25 mM potassium

glutamate, 1 mM MgSO_4 , 1 mM dithiothreitol and 20 mM tris-HCl buffer, pH 7.9) in a plastic Petri dish (35 mm diameter and 10 mm depth).

After the spermatozoa were treated with the extracting solution for about 30 s, 1 mM of ATP was added to the medium to reactivate them. For experiments of motionless demembranated flagella, the demembranated flagella reactivated with 1 mM ATP were put into solution containing 1 mM calcium chloride or 50 μM sodium orthovanadate (Wako Pure Chemical Industries, LTD., Tokyo).

The prepared sperm suspensions were put into a trough (T in Fig.2). One of the spermatozoa was fixed at its head to the tip of a braking micropipette (P) (cf. Hiramoto 1974) sucking the sperm head as shown in Fig.3. The orientation of the spermatozoon was adjusted by tilting and rotating the micropipette attached to an instrument collar (I) held with a micromanipulator (M_1) (Ernst Leitz GmbH., Wetzlar, W.Germany) so as to bring the entire length of the flagellum into the focal plane of the microscope. Since the micropipette was fixed to the instrument collar after passing through a hole set on the axis of the instrument collar, the spermatozoon at the tip of the micropipette was always in the microscopic field when the micropipette was rotated.

Observations of the flagella were made with a Nikon phase contrast microscope with BM 20 x objective at a magnification 200 x. In the microscopic observation, a high-pressure mercury arc lamp (Model HH 100T Tiyoda Kogaku K.K., Tokyo) was used for illumination. In the photographic recording,

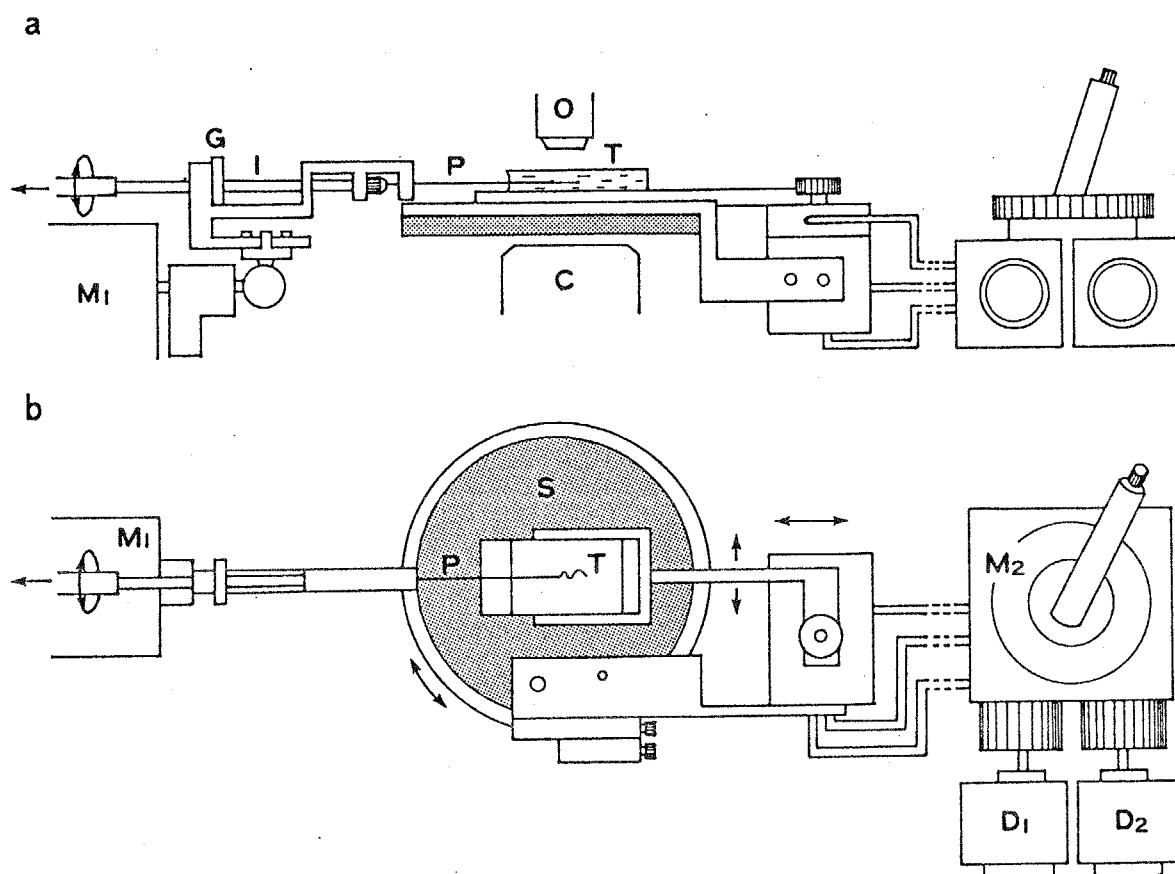


Fig.2. Experimental setup.

(a), front view; (b), plan view. C, long-focal-length condenser; D_1 and D_2 , motors; G, graduator measuring rotation angle of micropipette; I, instrument collar holding a micropipette; M_1 and M_2 , micromanipulators; O, objective lens; P, micropipette; S, microscope stage; T, trough.

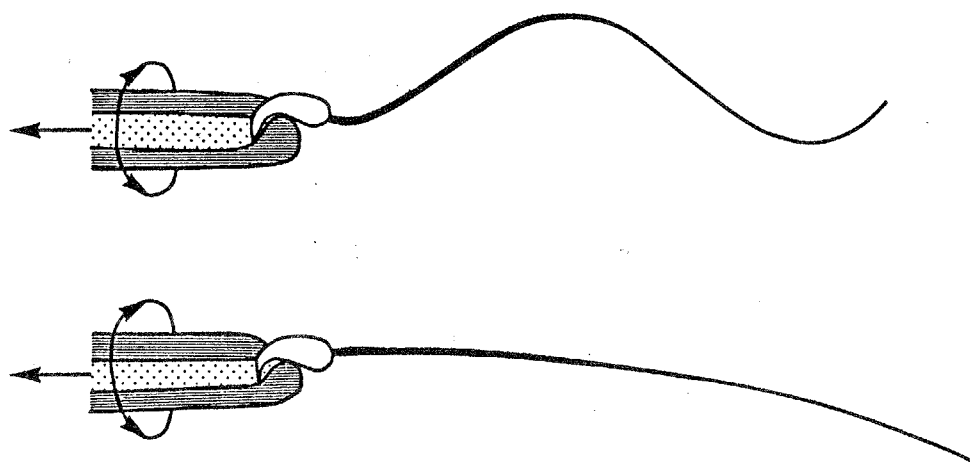


Fig.3. Technique for fixing a golden hamster spermatozoon at its head to the tip of a micropipette.

the flagellum was illuminated with stroboscopic xenon flashes at the rate of 50 Hz (Model 100 Chadwick-Helmuth Co., Inc., Monrovia, CA) and then images of the flagellum formed with the microscope were formed on Kodak Tri-X film moving at a constant speed, 1 m/s, after magnification with the microscope.

Analysis of the photographic records of flagella was carried out by tracing the image of the flagellum on a sheet of paper after a 428 x magnification with Goko LP-6 PROFILE PROJECTOR (Sansei Koki Co., LTD., Tokyo). Measurements were made directly with these traces.

The curvature of the bend in flagella was measured by finding a circle fitting to the trace of the bend among many template circles.

Effects of stationary stream of the medium on the flagellar movement

In flagellar movement of mammalian spermatozoa, bending waves were initiated at the base of the flagellum and propagated toward the tip. Because the bending of the flagellum occurred in a definite plane, the image of the flagellum which was in focus over its entire length could be obtained if the spermatozoon was observed from an appropriate direction as shown in Fig.4.

As shown in Fig.4a, when a stream was applied in the

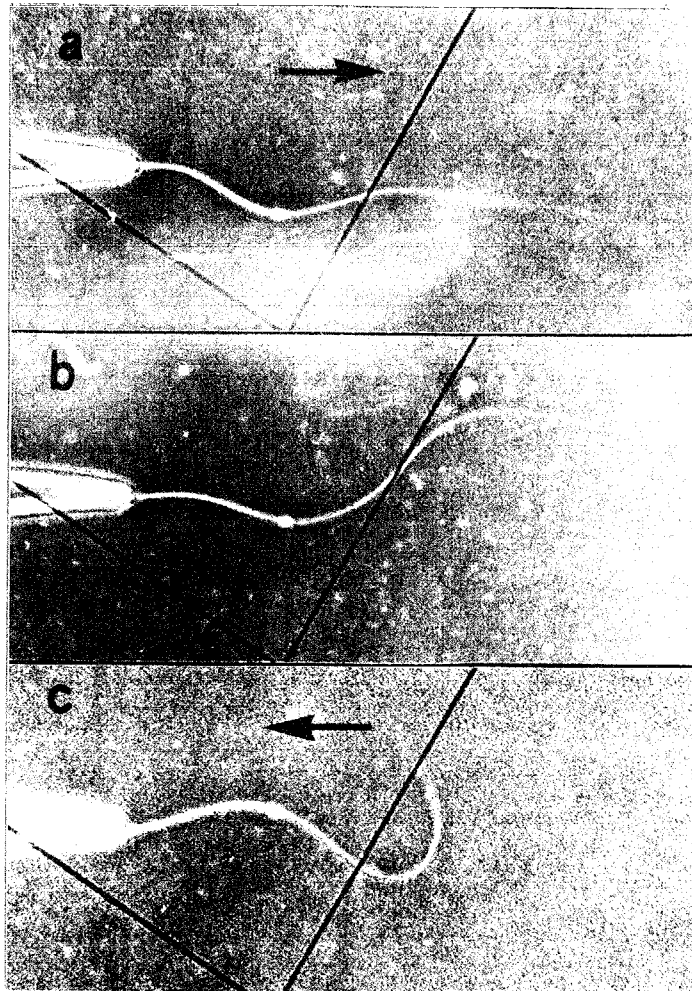


Fig.4. The deformation of the flagellar wave in a golden hamster spermatozoon. Arrows indicate the stream directions.

direction from the base to the tip of the flagellum, the wavelength increased and the amplitude decreased as if the waveform was stretched in the direction of the stream, and in consequence, the curvature of the bent portion of the flagellum decreased. When the speed of the stream increased, the curvature of the bend decreased and the wavelength increased, the flagellum became almost straight without motility.

When a stream was applied in the direction from the tip to the base of the flagellum, the wavelength decreased and the amplitude increased as if the waveform was compressed as shown in Fig.4c. As the speed of the medium increased, the wave was distorted and became non-planar.

When the micropipette holding the spermatozoon was rotated by 90° about its axis so as to make the beating plane of the flagellum perpendicular to the field plane of the microscope, parts of the flagellum in focus were observed as a train of spots moving toward the tip of the flagellum as shown in Fig.5a-c. The spots were continuously moving from the base of the flagellum toward the tip indicating the propagation of the bending wave. When the medium was moved in the direction perpendicular to the beating plane, the beating plane was bent by the stream as shown in Figs.5a'-c'. When the speed of the stream was increased, the flagellar beating deviated from the regular planar one. No difference in the degree of bending of the beating plane was found between streams of opposite directions provided that the absolute values of the stream speed were

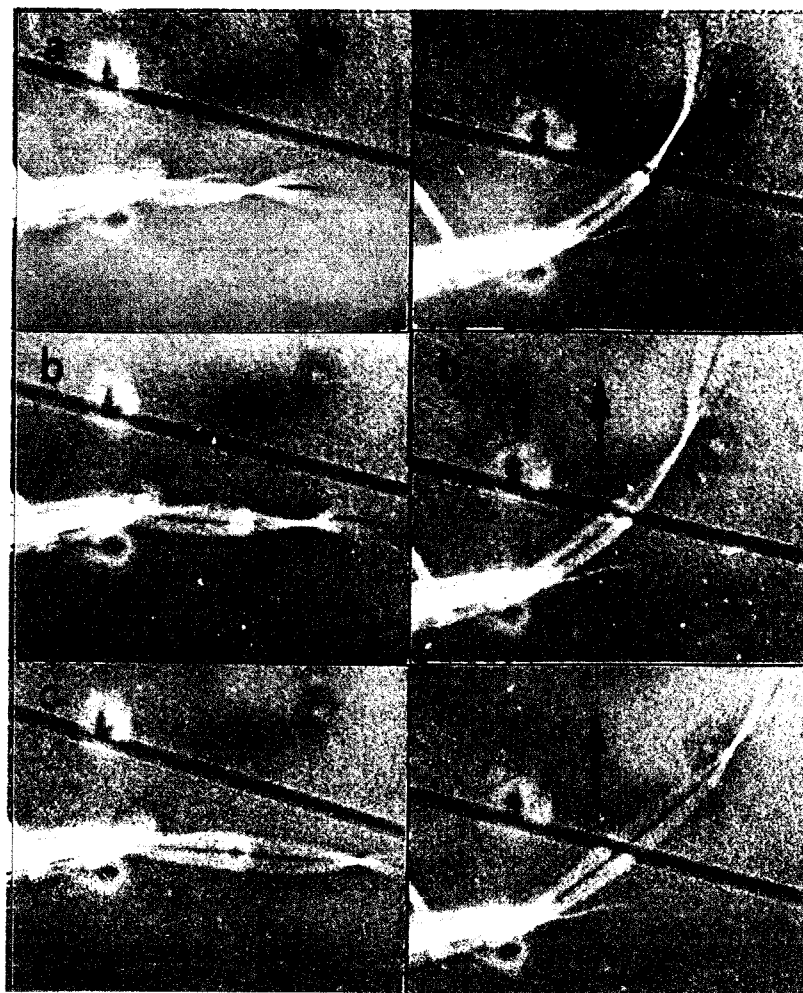


Fig.5. The deformation of the flagellar beating plane in a golden hamster spermatozoon when a stream was applied in the direction perpendicular to the beating plane. Arrows indicate the stream directions.

the same.

When reactivated by ATP, demembranated cauda epididymal spermatozoa exhibited vigorous movement like intact capacitated and activated spermatozoa as reported by Mohri and Yanagimachi (1980). Effects of stationary stream on reactivated demembranated flagella were similar to those of live flagella: The bending wave was "stretched" when the stream of medium was applied to the flagellum in the direction from the base to the tip of the flagellum and was "compressed" when the stream direction was reversed; and the beating plane of the flagellum was bent when the stream was applied in the direction perpendicular to the beating plane.

Procedure for calculation of flexural rigidity

In the present study, methods the same as those in sea urchin sperm flagella (cf. CHAPTER I) were used for calculation of the flexural rigidity of mammalian sperm flagella.

Flexural rigidity of sperm flagella

A. The flexural rigidity of beating flagella

The average flexural rigidity of flagella beating in Tyrode's solution was $6.4 \times 10^{-20} \text{ Nm}^2$ determined at point about 80 μm from the base (cf. Table I). No significant difference was found in the flexural rigidity between measurements using the stream from the base to the tip of the flagellum "stretching" the flagellar wave and the stream from the tip to the base of the flagellum "compressing" the flagellar wave.

The average flexural rigidity of beating flagella for bending in the plane perpendicular to the beating plane was $4.6 \times 10^{-19} \text{ Nm}^2$, 7 times that of beating flagella for bending within the beating plane (see Table I).

B. The flexural rigidity of motionless living flagella

The flagellum of spermatozoon fixed at its head to the tip of a micropipette was bent by the viscous resistance of the medium acting on the flagellum when a stream of the medium was applied in the direction perpendicular to the tangent at the base of the flagellum.

In spermatozoa which had lost their motility in Tyrode's solution containing 10 mM sodium azide, the flagellum was slightly curved in a position where only the reverse bend persisted.

The average flexural rigidity of living flagella immobilized with sodium azide was $6.9 \times 10^{-19} \text{ Nm}^2$ for bending within the plane containing the hook shape of the head, i.e. the beating plane when the sperm is activated and was $6.6 \times 10^{-19} \text{ Nm}^2$ for bending in the direction perpendicular

Table I. Flexural rigidity of golden hamster sperm flagella (10^{-19} Nm^2).

(mean)

	Motionless			Beating		
	Medium	a ¹⁾	b ²⁾	Medium	a ¹⁾	b ²⁾
Living flagella	10 mM NaN_3	6.9 ± 3.5	6.6 ± 1.8	Tyrode's sol.	0.64 ± 0.27	4.6 ± 2.2
	0 mM ATP	8.1 ± 4.6	7.4 ± 3.7	1 mM ATP	0.60 ± 0.22	4.0 ± 1.9
Demembranated flagella	1 mM ATP, 50 μM vanadate	0.95 ± 0.43				
	1 mM ATP, 1 mM CaCl_2	1.2 ± 0.7				

1) Bending in the beating plane.

2) Bending in the direction perpendicular to the beating plane.

to the above plane as shown in Table I. No difference in flexural rigidity was found by the difference in the bending directions in reference to the "beating" plane.

C. The flexural rigidity of reactivated demembranated flagella

The average flexural rigidity of beating demembranated flagella was $6.0 \times 10^{-20} \text{ Nm}^2$ as shown in Table I. No difference was found in the flexural rigidity determined by "stretching" the flagellar wave by stream flowing from the base to the tip of the flagellum from that determined by "compressing" by the stream in opposite direction.

The average flexural rigidity of reactivated demembranated flagella was $4.0 \times 10^{-19} \text{ Nm}^2$, 7 times that of beating flagella for bending within the beating plane (cf. Table I). These values are similar to those in intact beating flagella (cf. Table I).

D. The flexural rigidity of motionless demembranated flagella

The flexural rigidity of demembranated flagella was measured in ATP-free medium. The average flexural rigidity of motionless demembranated flagella was $8.1 \times 10^{-19} \text{ Nm}^2$ for bending within the beating plane and $7.4 \times 10^{-19} \text{ Nm}^2$ for bending in the direction perpendicular to the beating plane (cf. Table I).

E. Effects of vanadate on the flexural rigidity of the demembranated flagella

Addition of 50 μ M sodium orthovanadate to the medium immediately arrested the movement of reactivated flagella, which exhibit S shapes, with the principal bend at the proximal region after ceasing the movement.

The average flexural rigidity of motionless demembranated flagella in the medium containing 1 mM ATP and 50 μ M vanadate was $9.5 \times 10^{-20} \text{ Nm}^2$, which is 12 per cent of that of motionless demembranated flagella in ATP-free medium and similar to that of beating flagella for bending within the beating plane (cf. Table I).

F. Effects of calcium chloride on the flexural rigidity of the flagella

When 1 mM CaCl_2 was added to the reactivated cauda spermatozoa, flagellar movement became asymmetrical and gradually ceased. Most of such demembranated sperm were arrested showing C shapes in which only the reverse bend persisted.

The average flexural rigidity of motionless demembranated flagella in the medium containing 1 mM ATP and 1 mM CaCl_2 was $1.2 \times 10^{-19} \text{ Nm}^2$, similar to that of motionless demembranated flagella in the medium containing 50 μ M sodium orthovanadate (cf. Table I).

Discussion

It is noted in Table I that value of the flexural rigidity of the flagellum immobilized with 10 mM sodium azide are more or less the same as that in demembranated flagellum in ATP-free medium. This fact may be explained that azide-poisoned flagella are in rigor state because azide is an inhibitor of cytochrome oxidase. As mentioned above, the flexural rigidity of motionless flagella immobilized with vanadate, which inhibit dynein ATPase activity, was only 12 per cent of that of motionless demembranated flagella in ATP-free medium (see Table I). As mentioned in CHAPTER I, in the presence of MgATP^{-2} and vanadate, axoneme is in a relaxed state. The flexural rigidity of flagella of golden hamster spermatozoon determined in the present study are about ten times that of bull sperm flagella obtained by Lindemann et. al (1973). The mean values of total length and diameter of flagellum at the middle piece of the bull spermatozoon are 74 μm and 0.8 μm , respectively, (cf. Kojima 1972), whereas the mean values of those of a golden hamster spermatozoa are 200 μm and 1.2 μm . According to Phillips (1972), the size of the outer coarse fibers correlates positively with the stiffness of the spermatozoa. Therefore, it seems likely that the difference in the stiffness of the flagellum between bull and golden hamster is due to the difference in the size of the outer coarse fibers.

As shown in Table I, the flexural rigidity for the

bending within the beating plane is very small compared with that for the bending in the perpendicular plane in living beating flagella. Similar results were obtained in demembranated flagella reactivated with 1 mM ATP. In both cases, the flagellum is flexible more than seven times for the bending within the beating plane compared with that for the bending in the perpendicular plane. Because no difference in flexural rigidity of motionless flagella was found between the bending within the plane containing the hook-shape of the head and the plane perpendicular to it, this difference of flexural rigidity of the flagellum by the difference in bending direction may be closely related to the mechanism of the flagellar movement.

Summary

1. The stiffness (flexural rigidity) of golden hamster flagella was determined from their deformation when a stream of medium was applied and the bending moment acting of the flagellum caused by the viscous resistance of the medium.
2. The flexural rigidity of the flagellum beating in Tyrode's solution was $4.6 \times 10^{-19} \text{ Nm}^2$ for bending in the direction perpendicular to the beating plane and was $6.4 \times 10^{-20} \text{ Nm}^2$ for bending within the beating plane.
3. A similar difference in the flexural rigidity by the difference in bending directions was found in demembranated flagella reactivated with 1 mM ATP: The flexural rigidity was $4.0 \times 10^{-19} \text{ Nm}^2$ for bending in direction perpendicular

to the beating plane and $6.0 \times 10^{-20} \text{ Nm}^2$ for bending within the beating plane.

4. The flexural rigidity of living flagella immobilized in sodium azide was $6.9 \times 10^{-19} \text{ Nm}^2$ for bending within the beating plane and was $6.6 \times 10^{-19} \text{ Nm}^2$ for bending in the direction perpendicular to the beating plane.

5. The flexural rigidity of motionless demembranated flagella in ATP-free medium was $8.1 \times 10^{-19} \text{ Nm}^2$ for bending within the beating plane and was $7.4 \times 10^{-19} \text{ Nm}^2$ for bending in the direction perpendicular to the beating plane.

6. The flexural rigidity of motionless demembranated flagella in medium containing 1 mM ATP and 50 μM vanadate was $9.5 \times 10^{-20} \text{ Nm}^2$.

7. The flexural rigidity of demembranated flagella in medium containing 1 mM calcium chloride and 1 mM ATP was $1.2 \times 10^{-19} \text{ Nm}^2$.

MOVEMENT CHARACTERISTICS OF GOLDEN HAMSTER SPERMATOZOA

Introduction

Mammalian spermatozoa exhibit sequential changes in their motility characteristics during their passage through the male reproductive tract and during capacitation process in the female reproductive tract as reported by Mohri and Yanagimachi (1980): Hamster spermatozoa taken from the testis and caput epididymides are virtually immotile, while cauda epididymal and ejaculated spermatozoa are capable of active progressive movement. Capacitated spermatozoa has very vigorous motility characterized by whiplash-like beating of their flagella. When spermatozoa of these types were demembranated with Triton X-100 and exposed to ATP (and cAMP), all of them began active movement.

These changes in their motility characteristics are due to the change in the beating pattern of sperm flagella.

Mammalian spermatozoa seem to be suitable for analyzing the regulatory mechanism of flagellar movement. In addition, rodent spermatozoa possess sickle-shaped heads that allow us easily to determine direction of flagellar bending under the light microscope.

From an analysis of waveforms of golden hamster spermatozoa fixed by rapid freezing, Woolley (1977) concluded that the principal bend, which is more effective and persists for a longer period than the other during flagellar beating, occurs in the direction in which the head projection points,

and the reverse bend occurs in opposite direction.

In order to investigate the mechanism underlying the change in the beating pattern, it is important to describe the flagellar movement of the spermatozoa as exactly as possible. In the present study, golden hamster spermatozoa were used as material and the flagellar movement of testicular, caput epididymal, cauda epididymal and capacitated spermatozoa were recorded after holding them at their heads with a micropipette.

Material and Methods

The testis and caput and cauda epididymides of golden hamsters placed separately in 10 ml of albumin-saline [0.9% NaCl and 1 mg/ml bovine serum albumin BSA, Reheis Chemical Co., Chicago, Illinois, pH 7.0] were minced with fine scissors. The extruded sperm suspension was filtered through a double layer of tissue paper (Kimwipes, Kimberly-Clark Corp.) and centrifuged at 3000 rpm for 5 min. The sediment of 1 μ l was resuspended in 10 ml of Tyrode's solution.

Capacitation of the cauda epididymal spermatozoa was induced according to Yanagimachi (1978) as follows. One cauda epididymis was isolated from mature male and epididymal duct was punctured at several places using a fine sharp forceps in order to obtain undiluted sperm. Undiluted sperm was suspended in 10 ml albumin-saline in a centrifuge

tube and centrifuged at 3000 rpm for 5 min. The sperm pellet was resuspended in 10 ml fresh albumin-saline with gentle pipetting. The sperm suspension was passed through a glass bead column, which was prepared by placing 3 g of 0.25-0.3 mm glass beads in a funnel plugged with absorbent, in order to isolate highly motile spermatozoa. The resulting sperm suspension was centrifuged at 3000 rpm for 5 min again and the supernatant was pipetted out. Fresh albumin-saline of 0.3 ml was added to approximately 0.1 ml loosely packed sperm pellet at the bottom of the centrifuge tube.

The sperm suspension (20 μ l) was put into 0.3 ml of capacitating medium (124.8 mM NaCl, 2.68 mM KCl, 1.80 mM CaCl_2 , 0.49 mM $\text{MgCl}_2 \cdot 6\text{H}_2\text{O}$, 0.36 mM $\text{NaH}_2\text{PO}_4 \cdot \text{H}_2\text{O}$, 11.90 mM NaHCO_3 , 4.50 mM Glucose, 0.09 mM Na-pyruvate, 9.0 mM Na-lactate, 0.5 mM Taurine, 0.05 mM l-Epinephrine and 15 mg/ml bovine serum albumin), which was placed at the center of plastic Petri dish and was covered with warm (37°C) mineral oil. This preparation was incubated at 37°C in an incubator for 3-4 hours.

To prepare demembranated sperm flagella, 5 μ l of the sedimented spermatozoa obtained from the testis and caput and cauda epididymides were added separately to 0.2 ml of an extracting solution in a Petri dish. After the spermatozoa were treated with the extracting medium for 30 s at room temperature, 1 mM of ATP was added to the medium to reactivate flagella.

The prepared sperm suspensions were put into a trough. For motility observation, a spermatozoon was attached at

its head to the tip of a sucking micropipette held with a micromanipulator as shown in Fig.3 of CHAPTER II. The orientation of the spermatozoon was adjusted by tilting the micropipette and turning it about its axis so as to bring the entire length of the flagellum into the focal plane of the microscope. Observations were made at 37°C.

A Nikon differential interference microscope was used for observation. The images of the flagellar movement taken by a video camera (AVC-1550 Sony Corp., Tokyo) were recorded on a video tape by illuminating with stroboscopic flashes synchronized with the video camera.

Results

A. Flagellar movements of intact spermatozoa

The flagella of the intact testicular spermatozoa suspended in Tyrode's solution repeated weak movements with waves of very small amplitude for several hours as shown in Fig.1a. No propulsive movement was observed. As shown in Fig.1b, movement of the intact spermatozoa from the caput epididymis was similar to that of the testicular ones, except for slightly higher beat frequency. In contrast with the testicular spermatozoa, some of them showed very slow progression. On the other hand, the spermatozoa from the cauda epididymis showed vigorous movement as shown

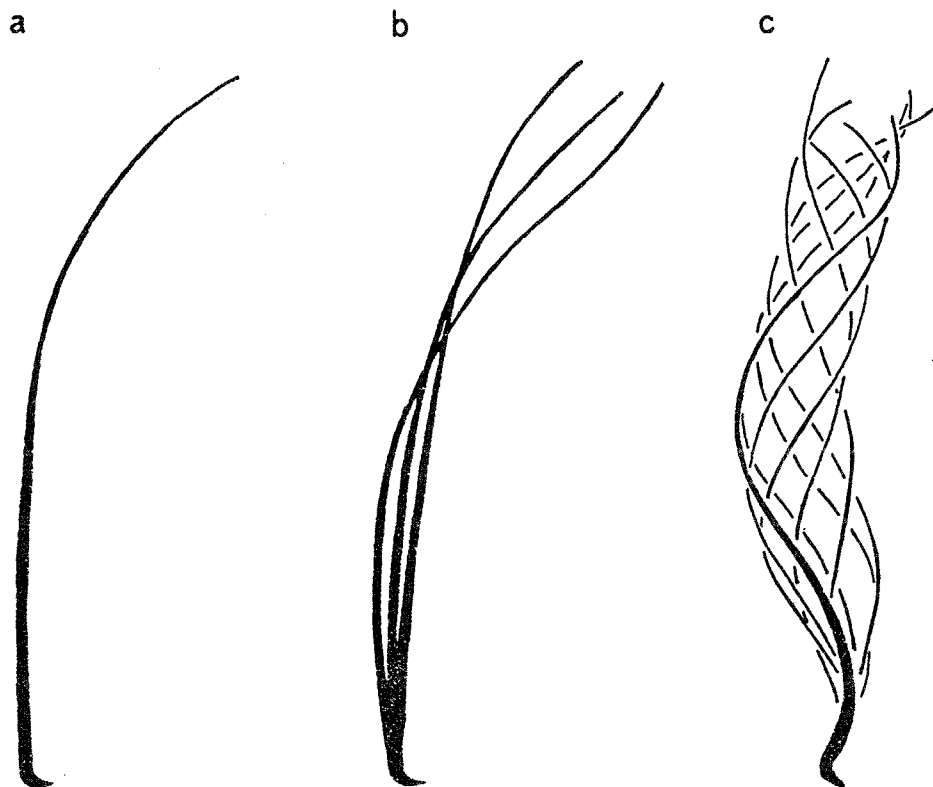


Fig.1. Typical flagellar beating patterns of intact spermatozoa.
(a) testicular spermatozoon; (b) caput epididymal spermatozoon;
(c) cauda epididymal spermatozoon.

in Fig.1c. In cauda epididymal spermatozoa fixed at their heads with the micropipette, it was possible to observe the flagella almost over their entire length, if their orientations were properly adjusted under the microscope as shown in Fig.2a. When the fixed head was rotated by 90°, the flagellum was seen as a straight train of spots corresponding to regions of the flagellum in focus.

The bending wave of the cauda spermatozoa was asymmetrical. The curvature of the "reverse" bend, which is shown in Fig.1a in CHAPTER II, was much larger than that of the "principal" bend. The mean values of beat frequency, amplitude and wavelength of the beating wave of the cauda epididymal spermatozoa were 12 Hz, 15 μ m and 80 μ m, respectively, as shown in Table I.

B. Flagellar movements of demembranated spermatozoa

When the testicular spermatozoa were demembranated with the extracting medium, they became motionless almost instantly. Upon exposure to 1 mM ATP, they began to move vigorously in a manner similar to that of intact spermatozoa extruded from the cauda epididymis. This vigorous movement lasted for about ten minutes and then, became asymmetrical with a low beat frequency as shown in Fig.3a. The mean values were 4 Hz for beat frequency, 20 μ m for amplitude and 95 μ m for wavelength.

The demembranated spermatozoa from the caput epididymis moved actively with waves of almost planar and large amplitude

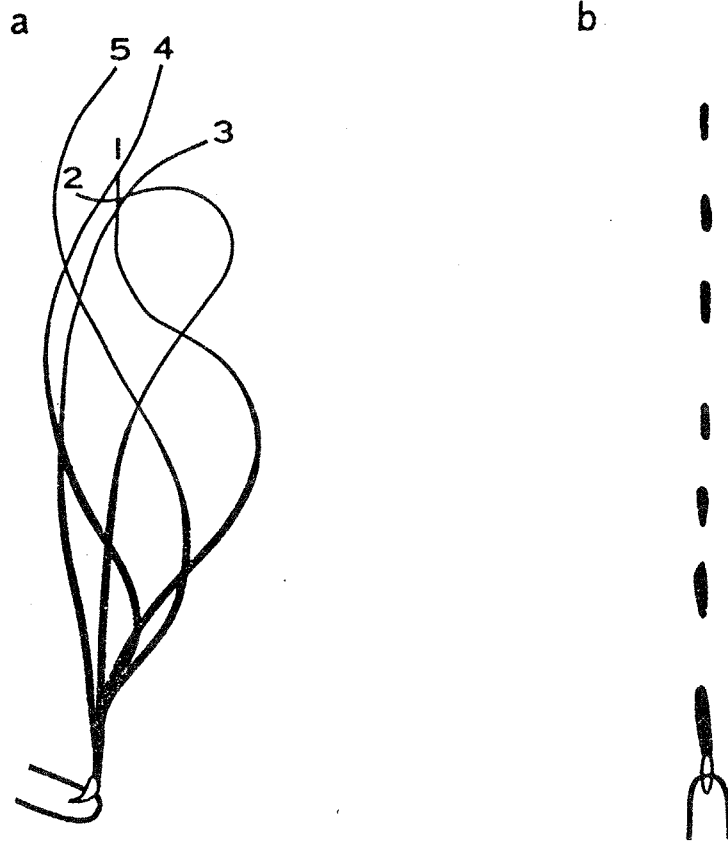


Fig.2. Typical flagellar beating patterns of intact spermatozoa from cauda epididymis during one beat cycle.

(a) The beating flagellum observed from the direction perpendicular to the beating plane. The numbers indicate the tracings of a flagellum at $1/60$ s intervals. (b) The beating flagellum observed from the direction parallel to the beating plane.

Table I. Movement characteristics of golden hamster spermatozoa.

		(mean)		
		Beat frequency (Hz)	Amplitude (μ m)	Wavelength (μ m)
Intact Spermatozoa (in Tyrode sol.)	Cauda Epididymal	12	15	80
	Testicular	4	20	95
Demembranated Spermatozoa (in 1 mM ATP)	Caput Epididymal	7	25	90
	Cauda Epididymal	6	28	100
Capacitated Spermatozoa	Cauda Epididymal	10	19	110

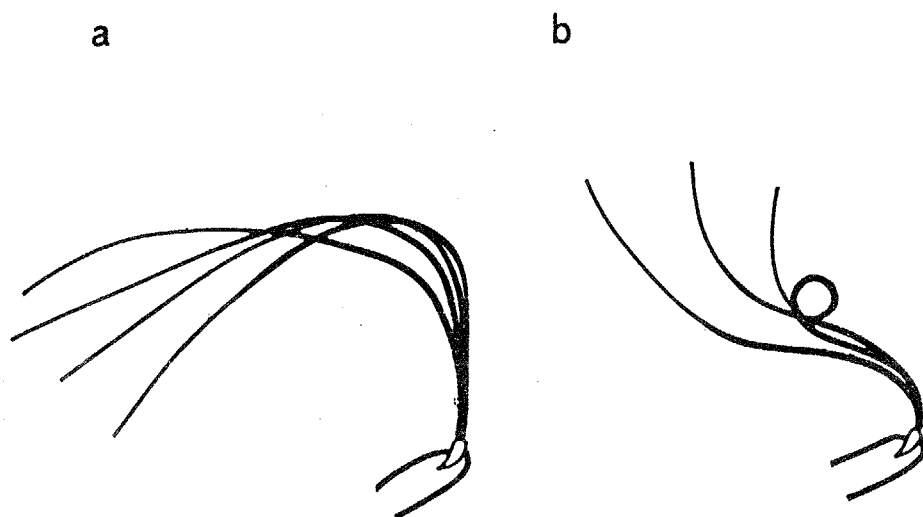


Fig.3. Typical flagellar beating patterns of demembranated spermatozoa reactivated with 1 mM ATP.
(a) testicular spermatozoon; (b) caput epididymal spermatozoon.

immediately after reactivating with ATP. The movement of the proximal region of the flagellum stopped within ten minutes, whereas the distal region of the flagellum continued to beat as shown in Fig.3b. In symmetrical bending wave of these spermatozoa, the mean values of beat frequency, amplitude and wavelength were 7 Hz, 25 μm and 90 μm , respectively. As shown in Fig.4, the demembranated cauda epididymal spermatozoa moved quite actively when ATP was added to the extracting medium, and such a movement continued for 20-30 minutes. The beat frequency, 6 Hz, was somewhat lower than that of the intact cauda spermatozoa, whereas the amplitude, 28 μm , and wavelength, 100 μm , were greater than those of the intact ones. The curvature of the "reverse" bend being much greater than that of the "principal" bend. When the bending wave was observed from the direction parallel to the beating plane, the displacement from the plane at the distal region of the demembranated cauda sperm flagellum was larger than that of the intact cauda sperm flagellum (cf. Fig.4b). There was a tendency that the displacement from the plane of the distal region was smaller in flagella showing symmetrical bending wave than in those exhibiting asymmetrical and irregular bending waves.

C. Flagellar movements of capacitated spermatozoa

As mentioned in Material and Methods, the spermatozoa from the cauda epididymis were suspended in the capacitating

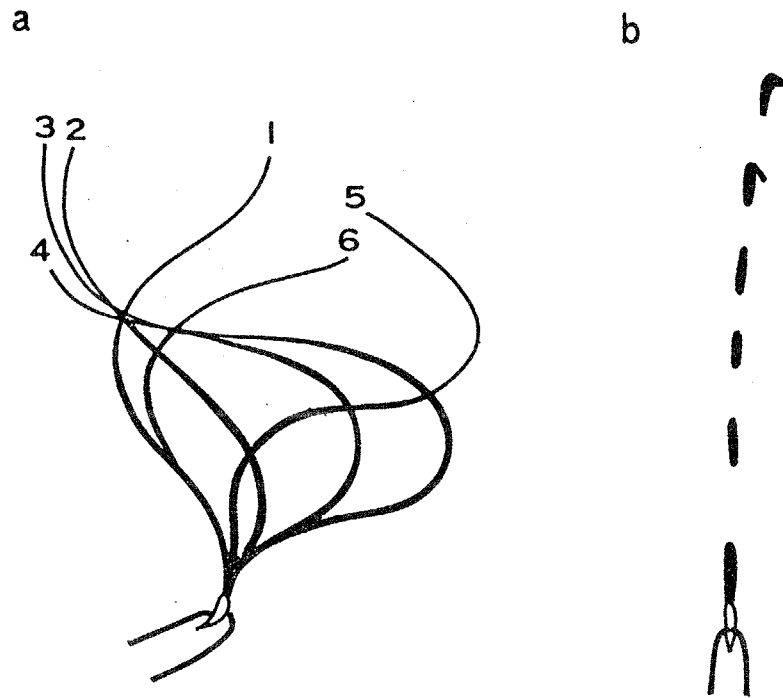


Fig.4. Typical flagellar beating patterns of demembranated cauda epididymal spermatozoa reactivated with 1 mM ATP during one beat cycle.

(a) The beating flagellum observed from the direction perpendicular to the beating plane. The numbers indicates the tracings of a flagellum at $1/30$ s intervals. (b) The beating flagellum observed from the direction parallel to the beating plane.

medium, and their movement was observed after capacitation (cf. Fig.5). The active movement continued for a few minutes and then rapidly ceased. The mean values of beat frequency, amplitude and wavelength were 10 Hz, 19 μ m and 110 μ m, respectively. These values lies between those of the intact and the demembranated cauda epididymal spermatozoa. Some of the capacitated spermatozoa, however, showed the wave pattern of a much greater amplitude (cf. Fig.5b), although such a pattern could be also observed in a few of the intact and demembranated cauda spermatozoa.

Table I summarizes the results of the beat frequencies, the amplitude and the wavelength of intact, demembranated and capacitated spermatozoa.

Discussion

From the geometry of the sperm flagella fixed by rapid freezing, Woolley (1977) reported that the bending plane twisted clockwise (viewed proximally). However, in the present study, when the cauda epididymal spermatozoon was fixed at its head with the micropipette, almost entire length of the flagellum could be observed suggesting planar nature of the beating. Moreover, when the flagellar movement was observed from the direction parallel to the beating plane, the image of the beating flagellum was seen as a straight train of points. These facts indicated that

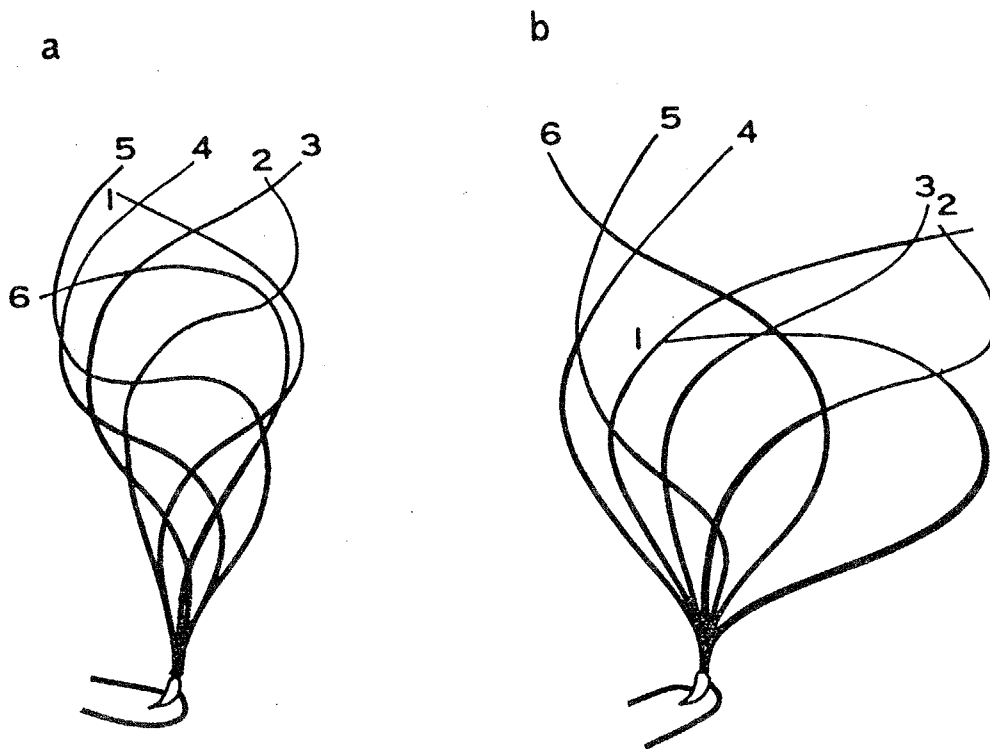


Fig.5. Typical flagellar beating patterns of capacitated spermatozoa during one beat cycle. The numbers indicates the positions of a flagellum at $1/60$ s intervals.
 (a) Usual beating pattern. (b) Beating pattern with a large amplitude.

the flagellar movement of the cauda epididymal spermatozoa is almost planar. However, when the bending wave of the demembranated flagellar movement of the cauda epididymal spermatozoa was observed from the direction parallel to the beating plane, the deviation from the planar nature at the distal region was larger than that of the intact one. Considering that the beat frequency of the intact spermatozoa was larger than that of the demembranated spermatozoa, the activity of the flagellar movement may be closely related to the mechanism of the generation of planar bending waves in flagella.

Mohri and Yanagimachi (1980) reported the beat frequencies of intact and demembranated golden hamster spermatozoa under various conditions. The values obtained by them were generally smaller than that of intact and capacitated spermatozoa obtained in the present study. The beat frequency of the sperm flagella measured stroboscopically in the present study may be more correct than that visually estimated by them.

Mohri and Yanagimachi (1980) concluded that golden hamster testicular and caput epididymal spermatozoa, which are both virtually immotile when they have intact plasma membranes, become motile after demembranization and ATP treatment. This may be interpreted as indicating that the motor apparatus, tubulin-dynein system, in these spermatozoa is already functionally assembled. The present study confirmed their conclusion.

In sea urchin spermatozoa, the principal bend has

a larger bend angle and beats toward outside if the spermatozoon swims along a circular path according to Gibbons and Gibbons (1972). If the same terminology is applied to hamster spermatozoa, the so-called "reverse" bend defined by Woolley (1977) would correspond to the principal bend in sea urchin sperm flagella.

Summary

In the present study, hamster spermatozoa taken from the testis and caput epididymis are virtually immotile, while cauda epididymal spermatozoa are capable of active progressive movement. Capacitated spermatozoa have vigorous motility characterized by whiplash-like beating of their flagella. When spermatozoa of these types were demembrated with Triton X-100 and exposed to ATP, all of them began active movement, although, the percentage of spermatozoa activated and the pattern and intensity of activation were somewhat different among these types of spermatozoa. These results suggest that the motor apparatus is functionally assembled before the spermatozoa leave the testis.

REFERENCES

1. Baba, S. A. (1972). J. Exp. Biol., 56, 459-467.
2. Bouchard, P., Penningroth, S. M., Cheung, A., Gagnon, C., and Bardin, C. W. (1981). Proc. Natl. Acad. Sci. U.S.A., 78, 1033-1036.
3. Brokaw, C. J. (1965). J. Exp. Biol., 43, 155-169.
4. Brokaw, C. J. (1977). J. Exp. Biol., 71, 229-240.
5. Brokaw, C. J., and Simonick, T. F. (1976). In Cell Motility (eds. Goldman, R., Pollard, T., and Rosenbaum, T.), pp. 933-940. Cold Spring Harbor Laboratory, New York.
6. Cohen, G., and Eisenberg, H. (1966). Biopolymers, 4, 429-440.
7. Fagen, J. B., and Racker, E. (1977). Biochemistry, 16, 152-158.
8. Fujime, S., Maruyama, M., and Asakura, S. (1972). J. Mol. Biol., 68, 347-359.
9. Gibbons, B. H., and Gibbons, I. R. (1972). J. Cell Biol., 54, 75-97.
10. Gibbons, B. H., and Gibbons, I. R. (1973). J. Cell Sci., 13, 337-357.
11. Gibbons, B. H., and Gibbons, I. R. (1974). J. Cell Biol., 63, 970-985.
12. Goldstein, S. F. (1979). J. Cell Biol., 80, 61-68.
13. Gray, J. (1955). J. Exp. Biol., 32, 775-801.
14. Gray, J. (1958). J. Exp. Biol., 35, 96-108.

15. Gray, J., and Hancock, G. J. (1955). J. Exp. Biol., 32, 802-814.
16. Hiramoto, Y. (1974). Exp. Cell Res., 87, 403-406.
17. Hoffmann-Berling, H. (1955). Biochim. biophys. Acta, 16, 146-154.
18. Katz, D. F., and Blake, J. R. (1975). In Swimming and Flying in Nature Vol. 1. (eds. Wu, T. Y. -T., Brokaw, C. J., and Brennen, C.), pp. 173-184. Plenum Press, New York.
19. Kojima, Y. (1972). In Mammalian Spermatozoa (ed. Iida, I.), pp. 146-179. Gakusosha, Tokyo. (in Japanese).
20. Lighthill, J. (1976). SIAM Rev., 18, 161-230.
21. Lindemann, C. B., Rudd, W. G., and Rikmenspoel, R. (1973). Biophys. J., 13, 437-448.
22. Mason, P. (1965). Kolloid-Z. Z. Polym, 202, 139-147.
23. Mohri, H. (1956). J. Exp. Biol., 33, 73-81.
24. Mohri, H., and Yanagimachi, R. (1980). Exp. Cell Res., 127, 191-196.
25. Okuno, M. (1980). J. Cell Biol., 85, 712-725.
26. Okuno, M., and Hiramoto, Y. (1979). J. Exp. Biol., 79, 235-243.
27. Oosawa, F. (1980). Biophys. Chim., 11, 443-446.
28. Phillips, D. M. (1972). J. Cell Biol., 53, 561-573.
29. Satir, P. (1965). J. Cell Biol., 26, 805-834.
30. Satir, P. (1968). J. Cell Biol., 39, 77-94.
31. Seames, A. E., and Conway, H. D. (1957). J. Appl. Mech., 24, 289-294.

32. Summers, K. E., and Gibbons, I. R. (1971). Proc. Natl. Acad. Sci. U.S.A., 68, 3092-3096.
33. Wainwright, S. A., Biggs, W. D., Currey, J. D., and Gosline, J. M. (1982). Mechanical Design in Organisms. Princeton University Press, Princeton.
34. Whittaker, E. T., and Robinson, G. (1926). The Calculus of Observations. 2nd ed., Blackie and Son, London.
35. Woolley, D. M. (1977). J. Cell Biol., 75, 851-865.
36. Yanagimachi, R. (1978). In Current Topics in Developmental Biology Vol. 12. (eds. Moscona, A. A., and Monroy, A.), pp. 83-105. Academic Press, New York.

ACKNOWLEDGMENT

I wish to express my thanks to Professor Y. Hiramoto for his valuable advices and encouragements in the course of the present work. Thanks are also due to Dr. H. Mohri of the University of Tokyo for some valuable suggestions.

I am grateful to Misaki Marine Biological Station of the University of Tokyo for supplying the echinoderms used as materials, and also to Dr. Y. Ishijima of Tokyo University of Agriculture for supplying male golden hamsters.

I wish to thank Dr. Y. Hamaguchi and Mrs. M. S. Hamaguchi for their kind suggestions.